TRANSMIT ANTENNA SELECTION FOR MULTIUSER MASSIVE MIMO

a thesis submitted to

The University of Kent

in the subject of electronic engineering

for the degree

of doctor of philosophy by research.

By

Ryan R Husbands

March 2018

Abstract

In massive multiple input multiple output (MIMO) systems, major challenges are present due to the large number of active antennas and radio frequency (RF) chains, such as increased power consumption and computation complexity. Transmit antenna selection (TAS) is being investigated as a solution to tackle these challenges. In this thesis, a dynamic transmit antenna selection technique is proposed which can maximize the sum rate of a multiuser (MU)-MIMO communication system. In order to satisfy the objective, the number of transmit antennas required is determined by remodeling it as a binary Knapsack Problem (KP) and then extending to a Multiple KP (MKP) for MU-MIMO. Furthermore, an improvement in the decision making is also proposed with the introduction of a flexible decision criteria, whilst reducing the structure of the MKP to resemble that of a single binary KP. Additionally, comparisons of the KP based algorithms are done with two low complexity techniques, which are the sequential selection algorithm and random selection algorithm. Results show that the KP based techniques outperform these low complexity techniques. The modified binary KP algorithm is also superior to that of the MKP, as it is not sensitive to solving as binary knapsack sub-problems. The proposed technique has good performance for different antenna selection measures and is suitable to ensure communication efficiency in future wireless communication systems.

Acknowledgements

First, I would like to express my gratitude to my supervisor Professor Jiangzhou Wang for his valuable advice and guidance during this PhD. He has been very helpful and supportive for all these years. I would also like to thank Dr Huiling Zhu for her helpful advice and insights with feedback on my research.

I am grateful to the School of Engineering & Digital Arts, and my supervisor in facilitating me with my research at a critical point. I would like to thank Relly, Mike, Cheng and Iulia. I would like to thank Natoya for her part and support in this journey. I would also like to thank the others who have contributed to this research.

I would like to thank my friends from back home for their constant support throughout my studies, Jason, Jason, Saffy, and Geoffrey. Last but not the least, I would like to thank my family: my parents and my brother for their constant support throughout my studies. Special thanks to my late grandfather.

List of Publications

1 R. Husbands, J. Wang, and H. Zhu, "Low Complexity Transmit antenna selection for Multiuser massive MIMO," submitted to IEEE Transactions on Wireless Communications.

2 R. Husbands, Q. Z. Ahmed, F. A. Khan, P. Lazaridis, and I. Glover, "Transmit antenna selection for massive mimo systems," Proceedings of the XXXI-Ind International Union of Radio Science General Assembly & Scientific Symposium (URSI GASS), (Montreal, 19-26 August 2017), August 2017.

3 R. Husbands, Q. Z. Ahmed, and J. Wang, "Transmit antenna selection for massive MIMO: a knapsack problem formulation," in IEEE ICC 2017 (ICC'17), (Paris, France), pp. 2313-2318, May 2017.

Contents

List of Tables

List of Figures

Abbreviations

4G Fourth Generation

5G Fifth Generation

AS Antenna Selection

AWGN Additive White Gaussian Noise

BBU Baseband Unit

CSI Channel State Information

DAS Distributed Antenna System

DL Downlink

DoF Degrees of Freedom

EE Energy Efficiency

FSPL Free Space Path Loss

i.i.d Independent and Identically Distributed

IMT International Mobile Telephone

ITU International Telecommunications Union

KP Knapsack Problem

LoS Line of Sight

MIMO Multiple Input Multiple Output

MKP Multiple Knapsack Problem

MMSE Minimum Mean Square Error

mmWave Millimetre Wave

MRT Maximum Ratio Transmission

MU-MIMO Multiuser Multiple Input Multiple Output

QoS Quality of Service

RF Radio Frequency

SE Spectral Efficiency

SINR Signal to Interference plus Noise Ratio

SNR Signal to Noise Ratio

SU-MIMO Single User Multiple Input Multiple Output

TAS Transmit Antenna Selection

UE User Equipment

ZF Zero Forcing

Chapter 1

Introduction

1.1 Motivation

Mobile communication has become intertwined with our daily lives and is slowly becoming officially recognized as an essential service. This is due to an exponential increase in the demand of the users. Mobile/wireless networks are under constant pressure to ensure customer satisfaction as these data demands are constantly increasing. Therefore, it is expected that in future networks the number of simultaneous users will be imperative, as wireless connectivity increases [1, 2]. The fifth Generation (5G) communications has been scheduled for commercialization in 2020 to ensure customer satisfaction as data demands are rapidly increasing [2]. In Fig. 1.1, the International Telecommunications Union (ITU) points out the requirements of International Mobile Telephone (IMT)-2020 known as 5G, with a comparison to IMT-Advanced known as 4G.

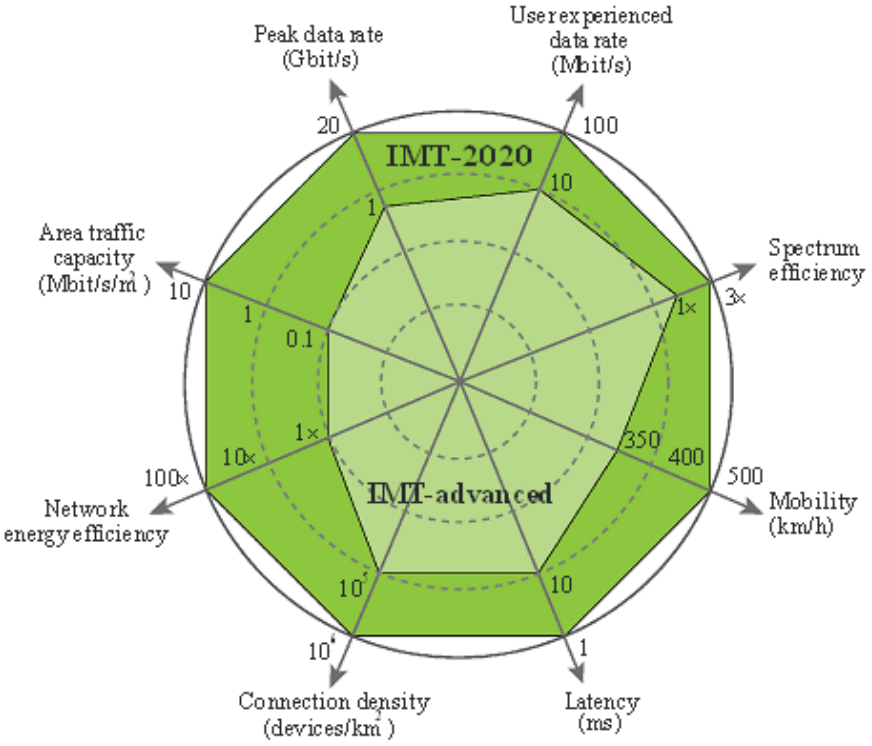

Figure 1.1: Enhancement of key capabilities from IMT-Advanced to IMT-2020 [1]

Fig. 1.1 illustrates the key requirements defined by the ITU. Some of these evaluation criterion of IMT-2020 contains the following performance measures: peak data rate, peak spectral efficiency, user experienced data rate, average spectral efficiency, area traffic capacity, low latency, connection density, energy efficiency, reliability, mobility, bandwidth, support of wide range of services, spectrum flexibility.

Enhanced mobile broadband has been identified to be intrensic in the 5G standardization process [3], where some of its key components are highly variable and/or higher data rates, and deployment and coverage. The aim of 5G wireless technology is to enable gigabit data rates, improved coverage, low latency, and increased connectivity. However, in order to achieve higher data rates and

improvements in capacity, advanced techniques are required. Some of these technological solutions that are important components for enabling higher data rates point towards the enhancement of the radio interface, such as advanced waveforms, modulation and coding, and multiple access schemes.

Approaches for enhanced spectral efficiency can be achieved via advances in physical layer techniques, spatial processing, and improvements on the network side through network densification. One key technique is to enable better spectrum utilization of the frequency bands, as there are large blocks of spectrum available in higher frequency bands. Another is the deployment of antenna arrays in a wireless system to improve coverage and spectral efficiency for wireless communications.

1.2 Critical 5G Wireless Technologies

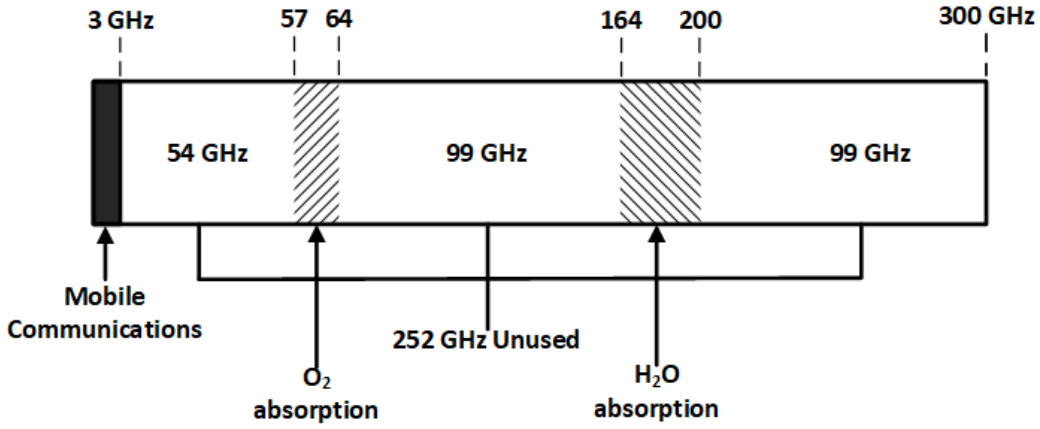

Figure 1.2: Radio Frequency Bands

1.2.1 Millimeter wave

As wireless communications market penetration continues to expand, the current microwave spectrum has become crowded. Current wireless communications operate in the 300 MHz to 3 GHz range [4, 5], as these bands were extremely favorable due to their propagation characteristics [6]. However, due to the limited spectrum, investigations into millimeter wave (mmWave) bands aim towards a solution. mmWave frequiences are within the 30 to 300 GHz range, and promise significant capacity increases over current cellular networks [7], and have demonstrated to achieve gigabit-per-second data rates. Researchers are studying advanced techniques which can effectively exploit the high frequency spectrum, such as mmWave to fulfill these data demands [8].

1.2.2 Multiantenna Techniques

Multiantenna techniques enable wireless systems to exploit the spatial dimensions to enhance reliability and/or spatial multiplexing of multiple data streams [9].

MIMO

This technique is called multiple input multiple output (MIMO) by having antenna arrays at the transmitter and/or receiver. MIMO offers diversity, multiplexing gain [10] and power gains [11], which improves the reliability, supports the spatial multiplexing of both single and multiple users, and increases the energy efficiency through beamforming techniques. MIMO has been included in current wireless standards with a limited number of antennas (two to eight antennas), and has proved satisfactory for current demands. However, there is significant research interest in massive MIMO, in order to meet future data demands . Massive MIMO is the deployment of a large number of antennas, typically in the tens to hundreds. Massive MIMO offers many benefits such as better reliability of

the wireless link, higher data rates, and a better trade off between energy and spectral efficiency, when compared to conventional MIMO technology. Therefore, the crafting of massive MIMO may require considerable architectural changes, particularly in the design at the base stations, which leads to new deployments scenarios [6].

Distributed Antenna Systems

Distributed antenna systems (DAS) are used to extend coverage area [12], improve spectral efficiency and reduce overall transmit power by reducing the distance between the transmitter and the receiver. DAS was originally an indoor technique [13], later it was adopted in outdoor systems. In outdoor DAS, antennas are geographically dispersed within a coverage area [14]. Each antenna array is connected to a baseband unit (BBU) through high-speed backhaul links, which enables coherent processing of the signal transmitted from the arrays [15]. Similar to MIMO, DAS can serve single or multiple users in the same time resource. Therefore, this arrangement can be called distributed MIMO [16, 17].

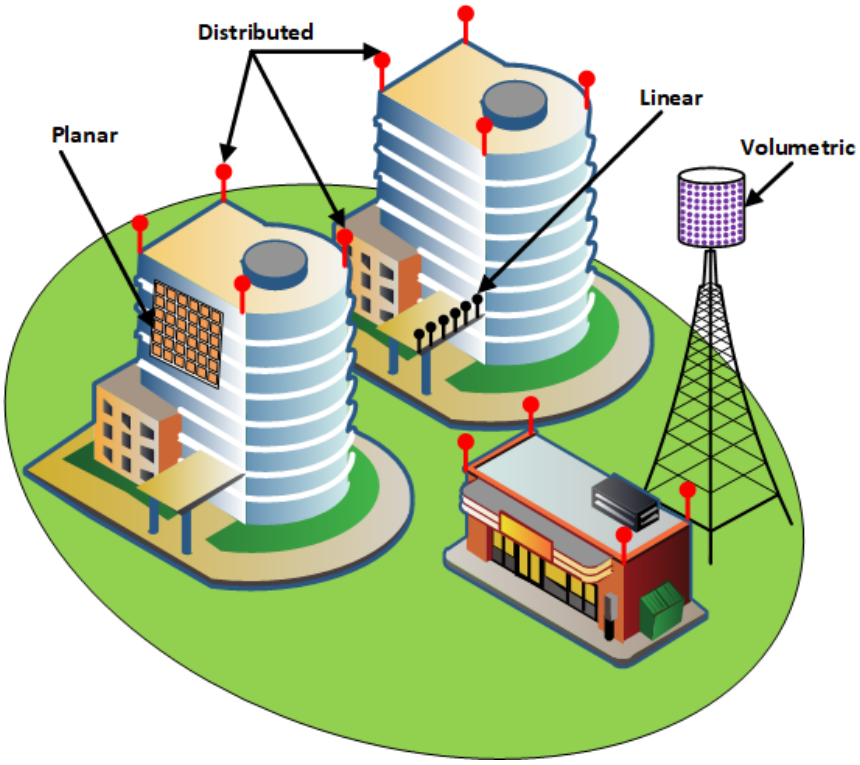

Figure 1.3: Massive MIMO deployments

Figure 1.3 depicts the different large scale multiantenna array deployments currently investigated: linear antenna arrays, planar antenna arrays, volumetric antenna arrays, and distributed antenna arrays. As shown in Figure 1.3, a large number of antennas could be dispersed within a cell, commonly referred to as large-scale distributed MIMO, or centrally deployed at a base station (BS), commonly referred to as massive MIMO.

1.3 Challenges of mmWave MIMO

The combination of mmWave and massive MIMO is welcomed as they provide critical relief to current wireless communications. mmWave proves to alleviate the over-crowding problem as it provides additional spectrum, and is a key enabler of massive MIMO. Massivie MIMO is invaluable as it provides large array gains [18, 19], which can combat the high pathloss suffered by mmWaves. However this combination presents many challenges [20], such as computational complexity and increased power consumption. While the use of massive MIMO allows for a reduction in transmit power, the number of radio-frequency (RF) chains becomes an issue. Therefore, power consumption becomes evident, since radio-frequency (RF) chains are accountable for 50- 80% of total power consumption [21], and they increase in proportion to the number of antennas[22, 23].

The energy efficiency (EE) is an important design criterion, considering the benefits from mmWave MIMO. In order to enhance EE, energy consumption should be considered in the overall design. Therefore, minimizing the number of RF chains at the BS is an attractive strategy. Much work has gone into reducing RF chains, such as hybrid beamforming and antenna selection. Hybrid beamforming structures have been proposed, with a limited number of RF chains which is much smaller than the number of antenna elements [23, 24]. Antenna selection reduces the number of RF chains by selecting a subset of antennas M_S out of M BS antennas based on a predefined criteria, such power or rate. As the number of RF chains is reduced from M to M_S in AS systems, this results in reduced circuit power. The EE of a transmission can be improved by both reducing RF transmit power and saving circuit power. Therefore to enhance energy efficiency, the variation characteristics of different users can be exploited, such as each user's individual rate requirements.

Scaling up the number of antennas in a MIMO system to improve the performance of wireless transmission must be accompanied with increasing the number of RF components. However, deploying more RF components will lead to an increase in the total power consumption in the system. Therefore, to cope with this problem, antenna selection (AS) technology comes to reduce the cost and complexity of MIMO architecture, while keeping most of its benefits. Considerable algorithms based on technical and mathematical concepts have been proposed to achieve either transmit or receive antenna selection or joint transmit/receive antenna selection. Our research concerns with transmit antenna selection (TAS) for MIMO systems.

1.4 Contribution of Thesis

The objective of this thesis is to study communication efficient methods for 5G mmWave wireless communications in the downlink multiuser (MU-MIMO), considering TAS with per-antenna power constraint and per-user SINR constraint. We propose communication efficient optimization solutions for mmWave wireless communication systems with massive MIMO. The contributions of this thesis are summarized as follows:

- The BS communication efficiency which includes satisfying the variable rate requirement and minimum power consumption of the RF chains, and the sum rate maximization for a fixed transmit power has be formulated as an optimization problem for 5G wireless communication systems employing mmWave massive MIMO.

- Considering the combinatorial nature of this optimization objective problem, a suboptimal solution is proposed to enable communication efficiency of the system using the binary knapsack (KP) algorithm.

- To reduce the cost and complexity of the RF circuitry, the EE is maximized with the minimum number of RF circuitry by minimizing the consumed energy.

- A low complexity alternative for interference mitigation has been proposed to reduce the impact of multiuser interference on the system's performance. It is important to remove interference between antenna subsets as this can severely degrade the performance of a transmission.

1.5 Structure of Thesis

This remainder of this thesis is organized as follows:

- Chapter 2 presents mmWave frequencies and the challenges associated with propagation for wireless transmission in 5G. It discusses the various multi-antenna techniques and channel capacity. It provides an overview of MIMO systems for wirless communications and the techniques to transmit data. It covers the concepts of mmWave transmissions and challenges. The principles of MIMO communications are discussed. Then the combination of mmWave and massive MIMO is presented. The advantages and challenges are covered.

- Chapter 3 gives the mmWave MIMO architecture and system model. A massive MIMO channel model is developed to determine the channel between the BS and the UE for us to study the antenna selection problem. The antenna array is also presented. It studies the impact of mmWave propagation along with beamforming. Antenna array processing via beam pattern analysis is also illustrated.

- Chapter 4 studies TAS for single user mmWave wireless systems.In this thesis, a transmit antenna selection algorithm is developed which satisfies a

quality of service (QoS) for a given user. TAS to find the minimum number of BS transmit antennas required is studied. The impacts of the number of antennas selected for a desired QoS is analyzed.

- Chapter 5 studies multiuser TAS for mmWave MU-MIMO. TAS for power minimization in massive MIMO is studied. Also the massive MIMO rate maximization problem for a fixed power requirement in relation to the subset size is studied. The impact of assigning individual subsets per user is presented. It also compares other low complexity algorithms for TAS. The impacts of power consumption and energy efficiency gains are analyzed, along with iterference suppression.

- Chapter 6 gives the conclusions of this thesis and presents possible future work.

Chapter 2

mmWave MIMO: Literature Review

2.1 Introduction

This chapter provides background information on mmWave propagation characteristics. The propagation of mmWaves are unique due to its short wavelength, and it is important to understand these fundamental characteristics to develop signal processing techniques for transmission in the mmWave bands. The Friis formula for free space path loss (FSPL) is described to show the dependence on the carrier frequency and distance, which clarifies the requirements of mmWave systems. Then, a description of the blockage effects on mmWave which is more severe when compared to lower frequencies due to the poor diffraction and high penetration loss, and the effects of weather and atmospheric conditions are described.

2.2 mmWave

The signal processing of mmWave is of significant interest [4], due to the different propagation environments, which presents new challenges when compared to sub-6 GHz wireless communication systems. The major drawback of mmWave propagation is the high path loss due to higher carrier frequencies of 30-300 GHz. With the lack of commercial activity, but some unregulated systems currently operating in a fragment of this band, attention has now shifted towards this underutilized spectrum [25, 26, 27]. However, mmWave propagation models are still maturing with extensive measurements but there are few analytic models [28, 29, 30]. Therefore, the propagation characteristics of mmWave frequencies are of significant concern, due to its high sensitivity and vulnerability to obstacles in its path.

2.2.1 mmWave Path Loss

The free space path loss (FSPL) can be used to predict the radio frequency (RF) attenuation over distance for transmission, which is inversely proportional to the square of the carrier frequency, this relationship is given by

$$P_r = P_t G_r G_t \left(\frac{\lambda}{4\pi d} \right)^2, \tag{2.1}$$

where P_t is the transmit power, P_r is the received power, d is the relative distance between the transmitter (Tx) and the receiver (Rx), λ is the wavelength, and G_t and G_r are the transmit and receive gains. Therefore, (2.1) implies that the pathloss increases inversely with the wavelength squared. To properly evaluate the performance of wireless communication systems, it is critical to understand the propagation environment. However, all propagation losses other than FSPL are not included in this term.

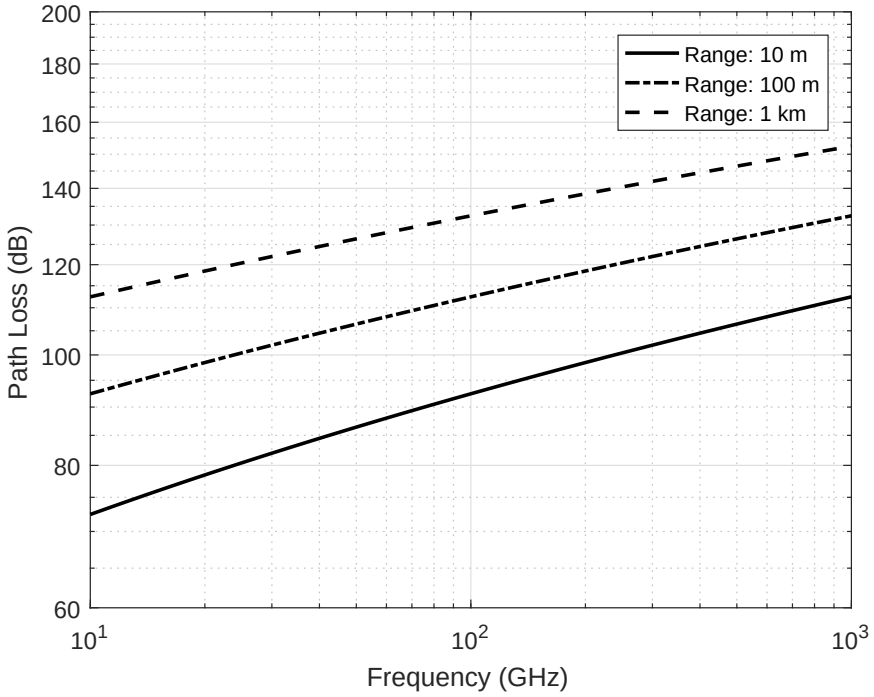

Figure 2.1: Free space path loss for mmWave frequencies

2.2.2 Atmospheric and Weather Losses

The FSPL model describes only part of the signal attenuation. Signals can experience additional path losses along the propagation path within the atmosphere. Atmospheric gaseous losses for mmWave transmission are due to oxygen molecule and/or water vapor adsorption. This oxygen or water vapor absorption result in band limited high attenuation causing signals to have shorter propagation distances. Rain is another concern regarding mmWave propagation, since raindrops are roughly the same size as the radio wavelengths.

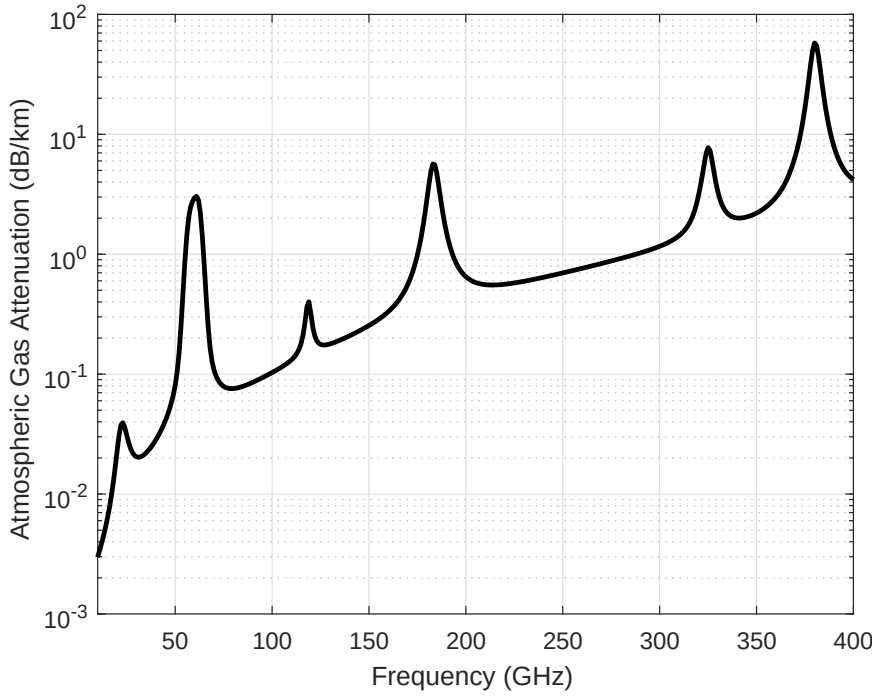

Figure 2.2: Atmospheric and molecular absorption at mmWave frequencies

Figure 2.2 illustrates the propagation loss due to atmospheric gases varies with the frequency, according to ITU model in [31]. It can be seen that signals interact with particles in the air and lose energy along the propagation path. The $57-64$ GHz band is an oxygen absorption peak, and the $164-200$ GHz band is a water vapor absorption peak. Nevertheless, beyond those absorption peaks, the spectral regions of mmWave are not heavily affected by gaseous losses.

Additional losses at mmWave frequencies can be attributed to reflection, which greatly depends on the material and surface. Reflection reduces the range of mmWave, but it enables non-line-of-sight (NLOS) communication. mmWaves suffer from high penetration losses as the signals do not penetrate solid materials well, as compared to lower frequencies which can penetrate most buildings easily. There are high levels of attenuation for certain building materials such as brick and concrete, which reduces the chances of outdoor to indoor communication at

mmWave. However, some signals might reach inside the buildings through glass windows and wood doors. Foliage losses for mmWaves are significant and can be a limiting impairment for propagation in some cases. An empirical formula to calculate the propagation through foliage was developed in [32].

2.3 Solution to mmWave Attenuation

It is known that an antenna with a larger aperture has a larger directivity than a smaller one. Therefore FSPL at mmwave can be accounted for by the decrease in the effective aperture as the carrier frequency increases. Since the antenna gain is proportional to the square of the frequency, it was pointed out in [7] that for a fixed physical aperture size, more antennas can be packed into the same area for shorter wavelengths. The transmission loss of mmWave is credited to FSPL, due to the fact that wavelength decreases with the increase in carrier frequency. Since smaller cell sizes are applied to improve spectral efficiency today [33], the rain attenuation and atmospheric absorption do not create significant additional path loss for short propagation distances. mmWave communications can be mainly used for indoor environments [34], small cell [35] or wireless backhaul [29, 36]. Therefore, mmWave communications will either be short range or require large antenna arrays to increase the coverage, leading to the combined benefit of mmWave Massive MIMO [6].

mmWave frequencies can benefit from multiantenna techniques by increasing the number of antenna elements to compensate for propagation losses. Along with smaller cell sizes, since the rain attenuation and atmospheric absorption do not create significant additional path loss for short propagation distances. The use of multiantenna techniques, provide diversity and array gain in the wireless channel. MIMO communication systems are defined by the use of MIMO antennas

proved satisfactory for previous and current demands by achieving higher spectral efficiencies in communication systems. Therefore by increasing MIMO, commonly referred to as massive MIMO, the door is opened for a large variety of features [18]. MIMO systems typically involve the combination of antenna arrays, signal processing and wave propagation characteristics.

2.4 Multiantenna Techniques

In this section, a description of the general evolution of wireless communication systems from single antenna to multiantenna deployments is given. The best way to increase data rates over a communications link is to increase the overall received signal power for a given transmit power. An effective method is to increase the number of transmit and/or receive antennas. MIMO schemes that can attain benefits such as multiplexing gain, diversity gain, and beamforming gain, whilst employing low-complexity linear receivers.

2.4.1 Spatial Multiplexing

In spatial multiplexing systems, multiple independent data streams are simultaneously transmitted by the multiple transmit antennas, thereby achieving a higher transmission speed. The basic principle of spatial multiplexing can be summarized as follows. The source bit sequence at the transmitter side is split into $\min(M_T, M_R)$ sequences, which are modulated and then transmitted simultaneously from the M_T transmit antennas, and received with M_R receive antennas, using the same carrier frequency. The number of spatially multiplexing streams can be determined from the rank of the MIMO channel matrix. At the receiver side, interference cancellation is employed in order to separate the different transmitted signals.

2.4.2 Diversity

Diversity techniques are employed in the presence of fading, exploiting the presence of multiple propagation paths between the transmitter and receiver. This technique allows the receiver to have several replicas of the same transmitted signal, while assuming that at least some of them are not severely attenuated. Diversity gains be achieved by creating independently fading signal replicas in the time, frequency or spatial domain. Therefore, diversity relies on the signal to be transferred over several different paths, where multiple versions of the same signal may be transmitted and/or received and combined at the receiver.

- Transmit Diversity is performed at the transmitter with multiple transmit antennas transferring the signal over different propagation paths, and is complicated to perform. Symbols can be spread across the array with the application of delays [37]. Feedback data from the receiver to the transmitter can be adapted to take advantage of the multiple signal paths.

- Receive Diversity utilizes multiple receive antennas to attain different observations of the same signal. These variations can be combined to better detect the transmitted symbols. Diversity with multiple receive antennas can be achieved with different combining techniques [38].

2.4.3 Beamforming

Beamforming uses multiple antennas at the base station by focusing energy in a specific direction in space [39], in order to send or receive the same information across all antennas by varying the phase and/or amplitude on each antenna. Beamforming relies on the knowledge of the channel to exploit the antenna array. Therefore, if the directions of the different propagation paths are known, then beamforming techniques can be employed in order to direct beam patterns in the direction of the specified users. Significant signal-to-noise ratio (SNR) gains can

be achieved by capitalizing on the antenna array gain when focusing energy in the direction of a desired user, whilst reducing the energy towards other users. Also, beamforming can be used in order to reduce the co-channel interference or multiuser interference. It is an effective technique to reduce interference, increase coverage, and increase capacity.

2.5 Shannon's Capacity Formula

The maximum rate at which information can be communicated across a noisy channel with arbitrary reliability is given by,

$$C = \log_2(1 + \text{SNR}) \ \ \text{bps/Hz} \tag{2.2}$$

Expressing Shannon's capacity formula for a given channel with a bandwidth B, the maximum achievable transmission capacity can be expressed as

$$C = B \log_2(1 + \frac{P}{N_o B}) \ \ \text{bits/s} \tag{2.3}$$

where P is the received signal power and N_0 is the noise spectrum, assuming that the channel is white Gaussian, as the SNR is represented by $P/(N_o B)$. These equations can be adopted in the MIMO configurations.

2.6 MIMO

A MIMO wireless system is a communication link where the transmitter and the receiver are equipped with multiple antennas. Considering the link between the transmitter and receiver, in general terms the link can be represented as

$$\boldsymbol{r} = \boldsymbol{H}\boldsymbol{x} + \boldsymbol{n} \tag{2.4}$$

where $\boldsymbol{r}$ is the received signal, $\boldsymbol{H}$ is the channel between the transmitter and receiver, $\boldsymbol{x}$ is the data transmitted and $\boldsymbol{n}$ is the noise within the channel.

2.6.1 SISO to MIMO

A wireless communication link is called single input single output (SISO) when the number of transmit antennas, M, is equals to one ($M = 1$), and similarly at the receiver ($N = 1$). A single input multiple output (SIMO) configuration has a single antenna at the transmitter and multiple antennas at the receiver, whereas ($M = 1, N > 1$). Multiple Input Single Output (MISO) configurations have a multiple transmit antennas transmitter and a single receive antenna, whereas ($M > 1, N = 1$). Multiple input multiple output (MIMO) communications refers to multiple transmit antennas and similarly multiple receive antennas, hence ($M > 1, N > 1$).

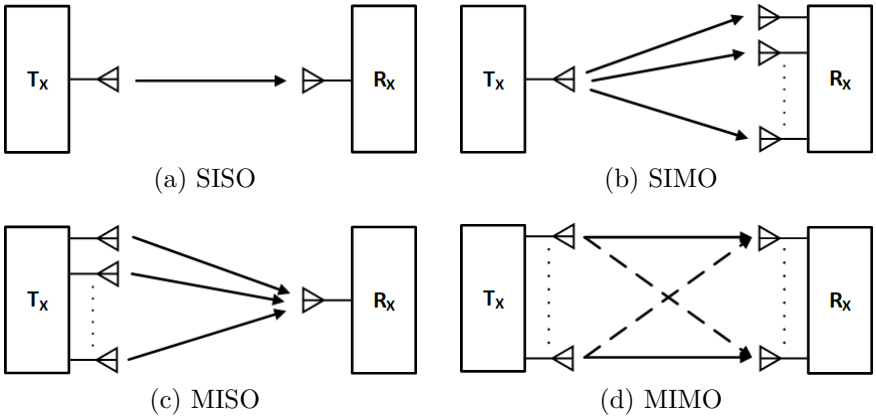

(a) SISO (b) SIMO

(c) MISO (d) MIMO

Figure 2.3: The figure depicts the different multiantenna configurations

2.6.2 Channel Capacity of SIMO, MISO and MIMO

SISO capacity is given as:

$$C = \log_2 (1 + \frac{|h|^2}{\sigma^2}) \tag{2.5}$$

where h_n is the normalized complex gain of the wireless channel.

SIMO capacity is given as:

$$C = \log_2 (1 + \frac{1}{\sigma^2} \sum_{n=1}^{N} |h_n|^2) \tag{2.6}$$

where h_n is the normalized complex channel gain associated with the nth receive antenna and N is the number of receive antennas.

MISO capacity is given as:

$$C = \log_2 (1 + \frac{1}{M\sigma^2} \sum_{m=1}^{M} |h_m|^2) \tag{2.7}$$

where h_m is the normalized complex channel gain associated with the mth transmit antenna and M is the number of transmit antennas.

MIMO capacity is given as:

$$C = \log_2 \left(\det \left[\boldsymbol{I}_N + \frac{1}{M\sigma^2} \boldsymbol{H}\boldsymbol{H}^H \right] \right) \tag{2.8}$$

where $\boldsymbol{H}$ is the $(M \times N)$ channel matrix associated with the N receive antennas and M is the number of transmit antennas. In (2.8), when there is no channel knowledge available at the transmitter, the best solution is to divide the power equally amongst the transmit antennas.

2.6.3 Precoding Techniques

Precoding is a multiantenna technique which supports multi-stream transmissions, and is known as beamforming.Precoding at the transmitter may take one of several forms, depending on the criterion or the method used to perform the

precoding. The simplest forms of precoding are linear and based on the following criteria.

- Maximum Ratio Transmission (MRT) or Hermitian precoding is a simple low complexity precoder given as

$$\boldsymbol{W}_{MRT} = \boldsymbol{H}^H \tag{2.9}$$

  This is a low complexity scheme, but more antennas are required at the BS to achieve a level of performance.

- Zeroforcing (ZF) is an interference mitigation strategy for MU-MIMO systems. The objective is to design one user's beamforming vector to be orthogonal to other selected users' channel vectors. The ZF beamforming to eliminate multiuser interference is given by

$$\boldsymbol{W}_{ZF} = \boldsymbol{H}^H(\boldsymbol{H}\boldsymbol{H}^H)^{-1} \tag{2.10}$$

- Minimum Mean Square Error (MMSE) precoding can trade interference reduction for signal power inefficiency. The MMSE pre-coder is given as

$$\boldsymbol{W}_{MMSE} = \boldsymbol{H}^H(\boldsymbol{H}\boldsymbol{H}^H + \sigma\boldsymbol{I})^{-1} \tag{2.11}$$

  where σ is the (SNR) at the MS. The MMSE aims to avoid the performance loss of the ZF precoding, when compared to the ideal channel capacity.

2.6.4 Mulituser MIMO

Multiuser MIMO is of significant interese as most communication systems deal with multiple users who are sharing the same radio resources. Figure 2.4 illustrates a typical MU-MIMO communication environment where a single BS serves

multiple UEs. Consider the MU-MIMO system as shown in Figure 2.4, the BS

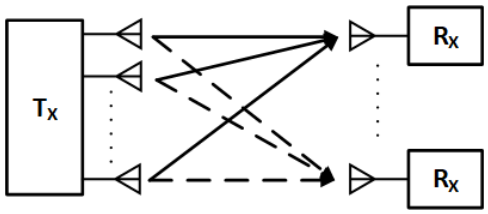

Figure 2.4: Multiuser MIMO system

has M antennas and each UE has N antennas. K independent UEs are served by the BS, and all data streams to each user should be independent. Therefore precoding techniques are essential to MU-MIMO transmissions to separate spatial streams among UEs. The downlink signal model can be represented as

$$\bar{\boldsymbol{r}}_k = \boldsymbol{H}_k \sum_{k=1}^{K} \boldsymbol{W}_k \boldsymbol{x}_k + \boldsymbol{n}_k \tag{2.12}$$

where $\bar{\boldsymbol{r}}_k$ is the received signal of the kth UE, $\boldsymbol{H}_k$ is the channel between the BS and kth UE, $\boldsymbol{x}_k$ is the data transmitted and $\boldsymbol{n}_k$ is the noise within the channel.

2.6.5 Mulituser Precoding

In MU-MIMO scenarios, the optimum transmission strategy for the downlink can be complicated due to the changing the transmit strategy for one user, which influences the SINR for every other user. The received signal of the receiving UEs is given by

$$\boldsymbol{y} = \boldsymbol{H}\boldsymbol{W}\boldsymbol{x} + \boldsymbol{n} \tag{2.13}$$

When a single BS with M antenna elements communicates simultaneously with K UEs, and assuming that the BS has complete CSI, interference between UEs can be effectively cancelled. Then, the received signal expressed in (2.12) at the

kth user can be expanded to

$$\boldsymbol{y}_k = \boldsymbol{H}_k \boldsymbol{W}_k \boldsymbol{x}_k + \boldsymbol{H}_k \sum_{j \neq k} \boldsymbol{W}_j \boldsymbol{x}_k + \boldsymbol{n}_k \tag{2.14}$$

In order to keep these data streams of different UEs apart is achieved by precoding. The downlink channel between K UEs

$$\bar{\boldsymbol{H}} = [\boldsymbol{H}_1, \boldsymbol{H}_2, \cdots, \boldsymbol{H}_k] \tag{2.15}$$

From Section 2.6.3, the following precoding matrices for MRT, ZF and MMSE beamforming are used.

$$\text{MRT:} \qquad \bar{\boldsymbol{W}} = \bar{\boldsymbol{H}}^H \tag{2.16}$$

$$\text{ZF:} \qquad \bar{\boldsymbol{W}} = \bar{\boldsymbol{H}}^H (\bar{\boldsymbol{H}} \bar{\boldsymbol{H}}^H)^{-1} \tag{2.17}$$

$$\text{MMSE:} \qquad \bar{\boldsymbol{W}} = \bar{\boldsymbol{H}}^H (\bar{\boldsymbol{H}} \bar{\boldsymbol{H}}^H + \sigma \boldsymbol{I})^{-1} \tag{2.18}$$

where

$$\bar{\boldsymbol{W}} = [\boldsymbol{W}_1, \boldsymbol{W}_2, \cdots, \boldsymbol{W}_k] \tag{2.19}$$

For the effective channel matrix in (2.15), interference free transmission can be achieved when precoding is applied and can be represented as

$$\boldsymbol{H}_k \boldsymbol{W}_j = 0 \ \forall j \neq k \tag{2.20}$$

Therefore it can be seen that the beamforming vectors are designed to completely cancel interference to others.

2.7 mmWave massive MIMO

2.7.1 Massive MIMO

Massive MIMO is an emerging technology which increases MIMO by orders of magnitude compared to current state of the art [40]. The main objective is to reap all the benefits of conventional MIMO but on a much larger scale. Massive MIMO employs the use of antenna arrays in the range of a few hundred antennas simultaneously serving many terminals in the same frequency resource. In future broadband networks, massive MIMO will be energy-efficient, secure, robust, and efficient in spectrum use. This can be achieved by a massive network densification with a significant increase in the number of antennas deployed per area, since spectral resources are scarce. The aim of massive MIMO is to reap all the benefits of conventional MIMO but on a much larger scale by using antenna arrays in the range of a few hundred antennas simultaneously serving many terminals in the same frequency resource [41]. Massive MIMO will be energy efficient, secure, robust, and efficient in spectrum use. This can be achieved by a massive network densification with a significant increase in the number of antennas deployed per area, since spectral resources are scarce.

Massive MIMO first appeared in [41], where the author showed that as the number of base station antennas grows without bounds, all the effects of uncorrelated noise and fast fading disappear. Also, the use of a large number of excess BS antennas serving a small number of users, allows for the simplest precoding techniques to be performed [42]. However, massive MIMO facilitates spatial multiplexing which relies on the BS having good knowledge of the channel. Two advantages of massive MIMO are increased capacity and improved energy efficiency. Therefore, more antennas means more degrees-of-freedom (DoF) that the propagation channel can provide [43]. However the number of antennas cannot

be infinitely large in a practical system due to size.

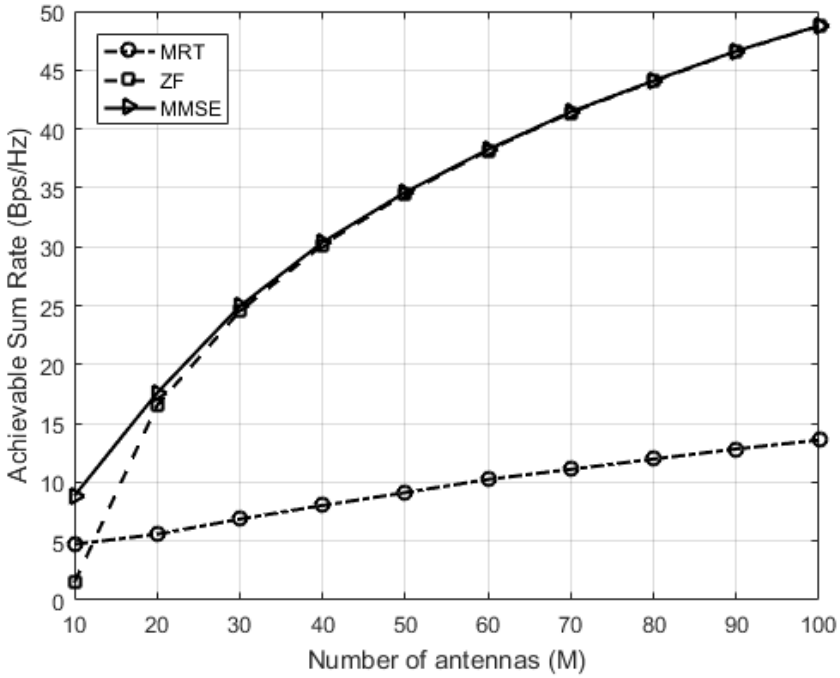

Figure 2.5: Sum rate for 10 UEs as the number of transmit antennas increase

Figure 2.5 illustrates the achievable downlink DL sum rates for 10 UEs. The figure shows the performance of the precoding schemes as the number of antennas increases. The MRT, ZF and MMSE precoding schemes in Section 2.6.3 are considered. The MMSE and ZF precoding schemes provide the same sum rates as the number of transmit antennas, M, increases. However, when $M < 20$ the ZF schemes suffers due to not enough DOF compared to the number of UEs.

2.7.2 mmWave MIMO

mmWave MIMO communications [44] has become one of the most attractive solutions for deployment and coverage in 5G wireless systems [45, 8], which can benefit from the large array gains [7] of massive MIMO, due to short wavelengths allowing deployment of dense antenna arrays in small physical spaces [46], since mmWave propagation is of significant concern [47, 48]. Massive MIMO promises an order-of-magnitude improvement in data throughput, link reliability, range, and transmit-energy efficiency [6, 18, 49], where mmWave can benefit from beamforming architectures with massive antenna arrays [50].

mmWave communications benefit from beamforming by having large antenna arrays and an increase in antenna aperture [33], along with a reduction in the downlink transmit power [51]. Beamforming is a technique used to focus energy in a specific direction to overcome pathloss [52], and is an efficient tool for improving both data rates and capacity. Therefore it can be used to combat the unfavorable effects of pathloss which significantly degrade the performance of mmWave communication systems. Many beamforming techniques have been developed by measuring the transmit output power using a variety of methods for the weighting vector, which ensures that the received signals are combined together in phase. The main objective of these beamformer techniques was to reduce the overall transmit power. However the impact of the RF components were neglected in the analysis, since the number of RF chains presents a problem [53].

2.7.3 Energy Efficiency

Energy efficiency in wireless communication techniques typically focus on minimizing the transmission energy only, which is reasonable in traditional wireless communication systems where the transmission energy is dominant in the total energy consumption. However in mmWave massive MIMO, the circuit energy consumption is comparable or even dominates the transmission energy. Therefore, a major concern is the power consumption, in mmWave MIMO systems, is that it relies on large numbers of antennas, and as the number of antennas increases the number of RF chains also increase [54]. RF chains are accountable for 50-80% of total power consumption at the BS [49]. The enhancement of energy efficiency requires the total energy consumption to be considered in the mmWave circuit design. Therefore, the energy efficiency of a transmission can be improved by both reducing RF transmit power and saving circuit power, as the variation characteristic of different users can be exploited for these improvements.

Since the circuit power consumption is now considered, which includes the energy consumed by all the circuit blocks within the transmission, different approaches are taken in order to minimize the total energy consumption. Many architectures have been investigated for mmWave MIMO throughout literature [55, 35, 56, 22, 11] with SE and EE in mind, such as the digital beamforming and hybrid analog-digital beamforming. Digital beamforming structures offer a higher DOF and better performance at the expense of cost and complexity, as it requires separate RF components for each antenna element. Hybrid beamforming structures have gained interest [36, 57], with a limited number of RF chains [56]. Architectures for connecting the RF chains in the hybrid processing that have been studied in the literature are fully connected and partially-connected [26, 23, 58]. In the fully connected, each RF chain is connected to all the antenna elements. In the partially connected only a subset of antenna elements are connected to each

RF chain.

The partially-connected architecture is more energy efficient and implementation-friendly since it can reduce the number of required phase shifters without significant performance loss. In particular, the authors in [57] demonstrate that the spectral efficiency of the hybrid-connected structure is better than that of the partially-connected structure and that its spectral efficiency can approach that of the fully-connected structure with an increase in the number of RF chains. Conversely in [59, 60], the authors show that fully digital beamforming can achieve better EE and still offer a superior performance, which is reinforced by the ongoing development in low-power circuits. Therefore, transmit antenna selection (TAS) can be employed to reduce overall system complexity in massive MIMO systems, resulting in an increase spectral efficiency (SE) or energy efficiency (EE).

2.7.4 Communication Efficiency

The deployment of mmWave and massive MIMO presents many challenges. [3] states that a 5G system should be communication efficient which is a measure of energy efficiency, and have the ability to be rate adaptive from the same device. Rate adaption for 5G refers to the flexiblity for both low and high data transmissions, and energy efficiency refers to the total power saved for a given transmission. In [61], the authors showed that as the number of base station antennas increases without bound, the transmit power of each antenna can be reduced proportional to the number of antennas. In massive MIMO, low complexity linear precoders are known to be close to optimal for massive MIMO, illustrated in Figure 2.5. However, the large number of antennas at the base station (BS) imposes a high computational complexity and high circuit power consumption. In efforts to mitigate interference in multi-user MIMO, this high complexity occurs with the matrix inverse of large matrices and the estimation of all the channels.

Concerning energy efficiency, there is a fundamental tradeoff between the number of active antennas, which is associated with circuit power consumption, where the power consumption scales linearly with the number of antennas [23, 54]. Traditional communication efficient techniques typically focus on energy efficiency which is the minimization of the transmit power, which is acceptable when the transmit power is large and the number of active RF chains is low. However, for massive MIMO when the transmit power is low, the circuit power consumption can be comparable or dominate the transmit power [62]. Therefore, a low complexity technique such as transmit antenna selection (TAS) can satisfy these requirements of 5G.

2.7.5 Transmit Antenna Selection

TAS is well-studied for traditional MIMO systems [54], with a few studies in mmWave MIMO [63]. TAS is an effective approach to ensure communication efficiency, saving power by turning off the inactive RF chains to satisfy a rate requirement. However, optimal antenna subsets are found by an exhaustive search which is impractical for massive MIMO. Therefore, it is critical to develop effective TAS algorithms for mmWave MIMO. Current studies in TAS mainly focus on the performance with a fixed number of selected antennas, energy efficiency or power minimization. The autors in [64] investigated the EE-SE tradeoff for massive MIMO with TAS. In [63], the authors proposed an iterative antenna selection algorithm for a mmWave MIMO system exploiting the strong line-of-sight (LoS) properties for beamforming gains, discrete stochastic approximation was used to quickly lock onto a near-optimal antenna subset, and [65] considered the uplink of large-scale MU-MIMO via an alternating optimization method.

An algorithm that jointly designs the antenna selection and baseband combining at the receiver for mmWave systems was studied in [58]. In [14], AS via convex optimization is used to determine the optimum antennas for a massively distributed MIMO system [66], which yields a fractional solution. The authors in [19] used measured data at 2 GHz to select the highest path gains. One method of selection relied on the Frobenius Norm of the channel state information (CSI) [67], which is impractical as it requires re-computation after each antenna element selection is made. The binary search method was employed in [68], which is comparable to the sequential selection. In [54], maximum SNR AS for massive MIMO systems was analyzed, and [69] performed TAS with non-orthogonal multiple acess (NOMA). In [68, 70, 71, 72], AS was performed resulting in a reduction in overall power consumption and hardware cost, while investigated EE [73]. The work in [74] suggested it is possible to increase sum rate by restoring any transmit antennas that were not selected. However, these works assigned selected antennas to all users, since multiuser (MU)-TAS is complex when associating each user with its own subset. The authors in [75] presented an algorithm which divides the total number of antennas into subgroups, then performs TAS on each subgroup. However this approach reduces the chances of having the best subset, as only the best antenna or set can be selected from each subgroup.

Research in reconfigurable antennas suggests the potential for fabricating large antenna arrays and using inexpensive high performance switches to adaptively select subsets [21], while retaining the advantages of massive MIMO [54, 76]. In [19], it was proposed to perform TAS using antennas connected to power switches. Considering the requirements for 5G, antenna subsets for each user offer better overall solutions. TAS offers the flexibility of assigning antenna subsets per user to satisfy individual rate or power requirements. TAS reduces power consumption as EE is dependent on number of active antennas. Currently, there is no efficient

method to find the global optimal solution other than the exhaustive search. In this thesis, the combinatorial optimizing problem of TAS is formulated as a binary knapsack problem (KP), capatilizing on its low complexity to implement as compared to convex optimization [77, 78, 79]. Binary KPs are non-deterministic polynomial-time (NP)-hard problems and are one of the most intensively and widely studied combinatorial optimization problems [77].

Methodology

In this thesis, antenna selection is done accordingly to the channel conditions, which represents a low-complexity method for determining antenna subsets. First, TAS was investigated for SU-MIMO based on a specified rate requirement. The performance of TAS and the number of antennas required against a threshold of full MIMO performance is investigated. The impact of SNR on selection was also investigated. Then an extension of TAS into MU-MIMO was done to include sum rate maximization and rate requirements for individual subset allocation in MU-TAS. Since MU-TAS is challenging when associating each user by its own subset, a low complexity method is presented finding a sub-optimal solution. Two variants for determining subsets are investigated, one variant is the maximum achievable system sum rate given a fixed number of RF chains which can be related to a fixed per UE power consumption, and the other is the minimization of total power consumed by satisfying a predefined rate requirement. Our goal is to improve EE with flexible and uniform user rates. Conventional approaches of MIMO maximize rates with a fixed transmit power or minimize transmit power for fixed rates. However, we factor the impact of the circuit power in the power consumption with TAS. The number of transmit RF chains at the MIMO transmitter can be reduced without compromising on the rate requirement using TAS. TAS can reduce RF hardware complexity, size, and cost. The algorithm determines if any given user rates can be delivered by simply selecting enough antennas.

2.8 Summary

The inclusion of mmWave frequencies alleviates the spectrum shortage. However mmWaves suffer from high pathloss. Therefore by going large with MIMO, a mmWave system can benefit from large array gains and increased diversity. Furthermore, massive MIMO systems allow for a better performance to be achieved without the need for additional transmit power or bandwidth. However, the large number of RF chains required is prohibitively high, and is reflected in the system complexity, hardware complexity and total power consumption. Therefore, massive MIMO may require major architectural changes, particularly in the design at the base stations, which leads to new deployment scenarios. However, TAS can be employed which reduces the impact associated of having multiple RF chains. Employing a smaller number of RF chains than the total number of transmit antennas, can reduce system complexity and total power consumption.

Chapter 3

mmWave System Design

3.1 Introduction

This chapter provides the channel model and tools that will be used in this thesis. This chapter discusses the capacity gains of the 3D beamforming in mmWave. The effect of the number of transmit antennas at the BS is based on the antenna array geometry. The principles for modeling the uniform liner array (ULA) and uniform rectangular array (URA) geometries are studied. The URA is used to produce the desired 3D beam. Both the horizontal and vertical element spacings are half wavelength, which is necessary for this analysis, since it is uniform spacing. A link budget analysis is given to evaluate the expected performance of the mmWave MIMO system performance.

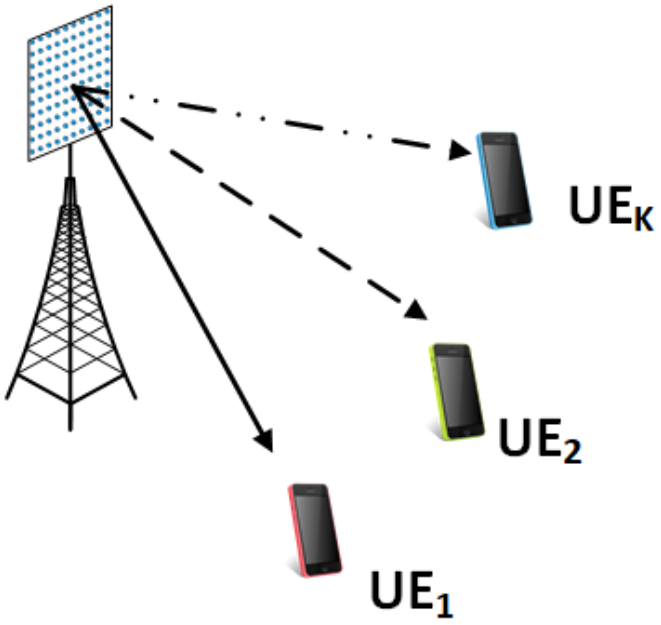

Figure 3.1: mmWave MIMO downlink transmission.

Consider the downlink of a 3D-MIMO system as shown in Figure 3.1. The system consists of a mmWave base station (BS) equipped with M antennas, which transmit data to K single antenna user equipments (UEs). The BS is equipped with a planar URA where the total number of transmit antennas M, is denoted by $M = M_h \times M_v$, equally spaced elements.

3.2 mmWave Channel Model

The 3D mmWave channel is the geometric based stochastic model as shown in [80, 81, 82]. The channel between the mth BS antenna element and the uth antenna element for the kth UE is given by

$$h_{u,m} = \alpha_k \cdot e^{(j\frac{2\pi}{\lambda}(\hat{r}^T_{rx,k,l}\cdot\bar{d}_{rx,u}))} e^{(j\frac{2\pi}{\lambda}(\hat{r}^T_{tx,k,l}\cdot\bar{d}_{tx,m}))} \tag{3.1}$$

where α_k is the complex channel gain and is explained as follows,

$$\alpha_k = \begin{bmatrix} F_{rx,\theta}(\Theta_k,) \\ F_{rx,\phi}(\Theta_k) \end{bmatrix}^T \begin{bmatrix} e^{(j\Phi_k^{\theta\theta})} & \kappa_k e^{(j\Phi_k^{\theta\phi})} \\ \kappa_k e^{(j\Phi_k^{\theta\phi})} & e^{(j\Phi_k^{\phi\phi})} \end{bmatrix} \begin{bmatrix} F_{tx,\theta}(\Psi_k) \\ F_{tx,\phi}(\Psi_k) \end{bmatrix}, \tag{3.2}$$

where $F_{rx,\theta}$, $F_{rx,\phi}$, $F_{tx,\theta}$, and $F_{tx,\phi}$ are field patterns of the receive and transmit antenna elements in the direction of θ and ϕ, respectively. $\Phi_k = (\theta_{k,ZOA}, \phi_{k,AoA})$ and $\Psi_k = (\theta_{k,ZOD}, \phi_{k,AoD})$. $\theta_{k,ZOA}$, $\theta_{k,ZOD}$, $\phi_{k,AoA}$, and $\phi_{k,AoD}$ are the zenith angle of arrival/departure (ZoA/D) and the azimuth angle of arrival/departure (AoA/D). κ_k represents cross polarization power ratio. $\Phi^{\theta\theta}$, $\Phi^{\theta\phi}$, $\Phi^{\phi\theta}$ and $\Phi^{\phi\phi}$ are random initial phases for four different polarization combinations. The terms $\hat{r}_{rx,k}$ and $\hat{r}_{tx,k}$ are the receiver (rx) and transmitter (tx) spherical unit vectors expressed in Cartesian coordinates as

$$\hat{r}_{i,k} = \begin{bmatrix} \sin\theta_{i,k}\cos\phi_{i,k}, \\ \sin\theta_{i,k}\sin\phi_{i,k}, \\ \cos\theta_{i,k} \end{bmatrix}^T \quad \text{for } i \in \Big[\text{tx,rx}\Big]. \tag{3.3}$$

$\bar{d}_{rx,u}$ and $\bar{d}_{tx,u}$, in (3.1), are the location vectors of receive and transmit antenna elements, respectively. Therefore, the miltiple input single output (MISO) channel vector for the kth user is given by

$$\boldsymbol{h}_k = \begin{bmatrix} h_{k,1} & h_{k,2} & \cdots & h_{k,m} \end{bmatrix}^T. \tag{3.4}$$

3.2.1 Array Geometry & Steering

The antenna array steering vectors, at the UE $\boldsymbol{a}_r(\theta_k^r, \phi_k^r)$ and the BS $\boldsymbol{a}_t(\theta_k^t, \phi_k^t)$, only depend on each antenna array's geometry. Assuming that all the array elements are isotropic sources, the beam patterns can be described by their array factors.

Uniform Linear Array (ULA)

The steering matrix is defined based on the antenna array's geometry and is therefore independent of the antenna element properties. A uniform linear array (ULA) is an easy case to illustrate, where a plane wave departing at angle θ has a different phase at each of the elements but the same amplitude. The array factor of the ULA with M elements, is given by

$$AF = \sum_{n=0}^{M-1} e^{jn\psi_i} \tag{3.5}$$

where ψ_i defines the array's orientation, and can be represented as follows:

$$\psi_i = \begin{cases} \beta d_x \sin\theta\cos\phi & d \text{ along } x \text{ axis, when } i = x \\ \beta d_y \sin\theta\sin\phi & d \text{ along } y \text{ axis, when } i = y \\ \beta d_z \cos\theta & d \text{ along } z \text{ axis, when } i = z. \end{cases}$$

$\beta = 2\pi/\lambda$, d is the inter-element spacing, and λ represents the wavelength of the mmWave system. The array vector of the ULA, $\boldsymbol{a}(\theta)$, is represented as

$$\boldsymbol{a}(\theta) = \begin{bmatrix} 1 & e^{j\psi_i} & \cdots & e^{j(M-1)\psi_i} \end{bmatrix}^T \tag{3.6}$$

Uniform Rectangular Array (URA)

The uniform rectangular array (URA) given in Figure 3.2, enables the beamforming system's ability to scan in three-dimensional (3D) space. The array factor of the uniform rectangular array (URA) in Figure 3.2, in the azimuth (az) and

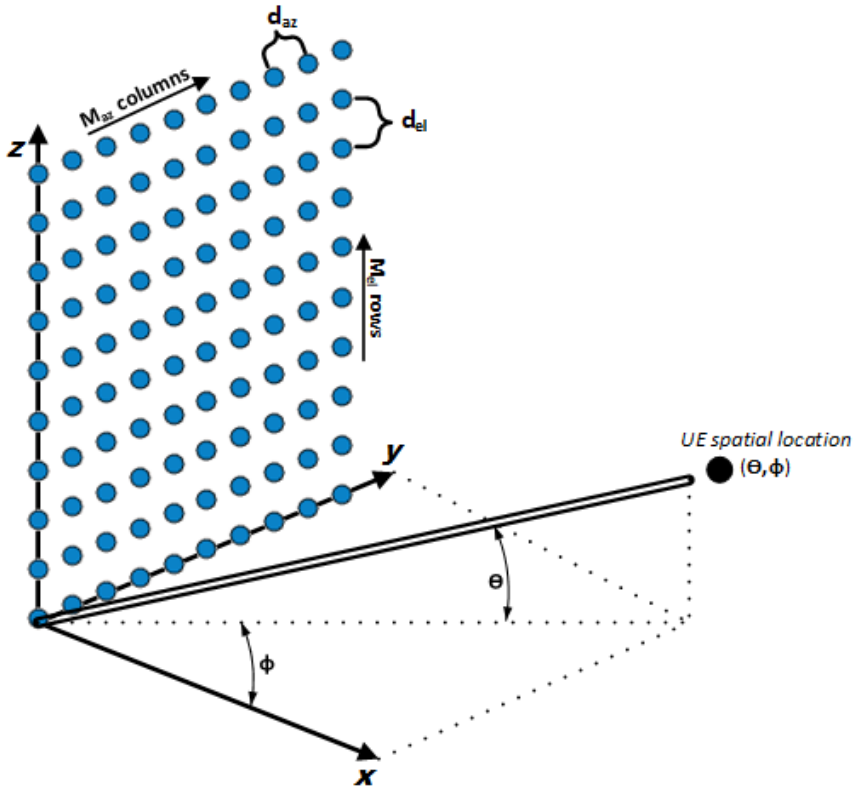

Figure 3.2: Uniform Rectangular Array (URA)

elevation (el) directions which are in (y-z) plane, and is given by

$$\begin{aligned} AF(\theta,\phi) &= AF_{\text{az}} \times AF_{\text{el}} \\ &= \sum_{l=0}^{L-1} e^{jl\psi_{\text{az}}} \times \sum_{\bar{n}=0}^{N-1} e^{jn\psi_{\text{el}}} \\ &= \sum_{l=0}^{L-1}\sum_{n=0}^{N-1} e^{j(l\psi_{\text{az}}+n\psi_{\text{el}})} \end{aligned} \tag{3.7}$$

where L and N are the number of elements in the azimuth and elevation directions, respectively. The URA steering vector can be extracted from the array factor taking the form

$$\boldsymbol{a}(\theta,\phi) = [1,\cdots,e^{j(\psi_{\text{az}}+\psi_{\text{el}})},\cdots,e^{j((L-1)\psi_{\text{az}}+(N-1)\psi_{\text{el}})}]^T. \tag{3.8}$$

3.3 Signal Model

The signal vector transmitted by the BS antenna array with beamforming can be defined as

$$\bar{\boldsymbol{x}} = \sum_{k=1}^{K} \boldsymbol{u}_k \boldsymbol{x}_k, \tag{3.9}$$

where $\boldsymbol{u}_k$ represents the beamforming vector and $\bar{x}_k$ represents the data symbol to be transmitted to the kth user. The following approach is adopted to find the beamformer weights. The BS beamformer weights $\boldsymbol{u}_k$ are designed to maximize the signal to noise ratio (SNR) at the kth user, and can be expressed as

$$\boldsymbol{u}_k = \frac{\boldsymbol{a}_k(\theta, \phi)}{\sqrt{\boldsymbol{a}_k(\theta, \phi)^T \boldsymbol{a}_k(\theta, \phi)}}. \tag{3.10}$$

In a single user scenario, the received signal at the selected kth user is given as

$$y_k = \boldsymbol{h}_k^H \boldsymbol{u}_k \boldsymbol{x}_k + \boldsymbol{n}_k, \tag{3.11}$$

where $\boldsymbol{h}_k$ is the channel between the BS and the kth UE, and $\boldsymbol{n}_k$ is the additive white Gaussian noise (AWGN) with zero mean and variance $\boldsymbol{\sigma}^2$. From (3.11), the signal to noise ratio (SNR) experienced by the kth user is given as

$$\mu_k = \frac{|\boldsymbol{h}_k^H \boldsymbol{u}_k|^2}{M \boldsymbol{\sigma}_k^2}. \tag{3.12}$$

The achievable rate at the kth user is given by

$$R_k = \log_2(1 + \mu_k). \tag{3.13}$$

3.4 Link Budget Analysis

In a mmWave wireless communications system, it is essential to know the SNR required to provide a certain level of performance at a specified rate or distance. Therefore, a satisfactory number of elements must be determined through an analysis of the system design parameters. Considering (3.11) and the FSPL given in chapter 2, the impact of the massive MIMO in mmWave frequencies can be studied.

Here we assume a simple line-of-sight free-space communication link with clear path between the transmitter and receiver, and a fixed B, applied to a 60 GHz system with the parameters defined in Table 3.1.

Table 3.1: Link budget Parameters

Spectral Bandwidth	1 GHz
Max radiated power	1 W
Antenna Structure	Planar - URA
Horizontal Elements	$1, 5, 10, 20$
Vertical Elements	$1, 5, 10, 20$
BS antenna gain	0 dBi
UE antenna gain	0 dBi
BS antenna height	15m
UE antenna height	ground plane
Thermal noise, N_0	174dBm/Hz
distance	$1 - 100$m

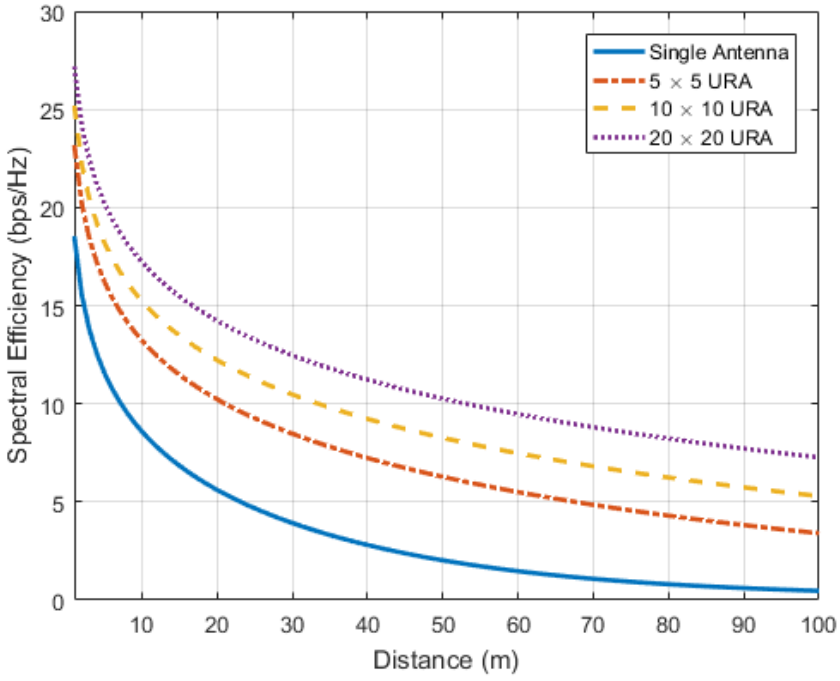

Figure 3.3: Comparison of single transmit and URA antenna configurations

Combining the parameters defined in (2.1), (2.3) and (3.12), the SE is given by

$$\text{SE} = \frac{C}{B} = \log_2 (1 + \frac{\text{SNR}}{M} \sum_{m=1}^{M} |h_m|^2), \tag{3.14}$$

and Figure 3.3 illustrates the achievable SE as the distance between the BS and the UE increases for different array sizes. It can be seen that as the distance increase the SE decreases, this is due to the FSPL attenuation of mmWave. A comparison was done with a single transmit antenna and three different size URAs. The URA sizes are $\{5 \times 5\}$, $\{10 \times 10\}$ and $\{20 \times 20\}$. However the unfavorable effects of FSPL are diminished as the size of the antenna array increases. The single transmit antenna achieved the lowest SE, whilst the largest $\{20 \times 20\}$-URA achieved the highest.

3.5 Beam Pattern Analysis

It is important to understand the radiation properties of antenna arrays.

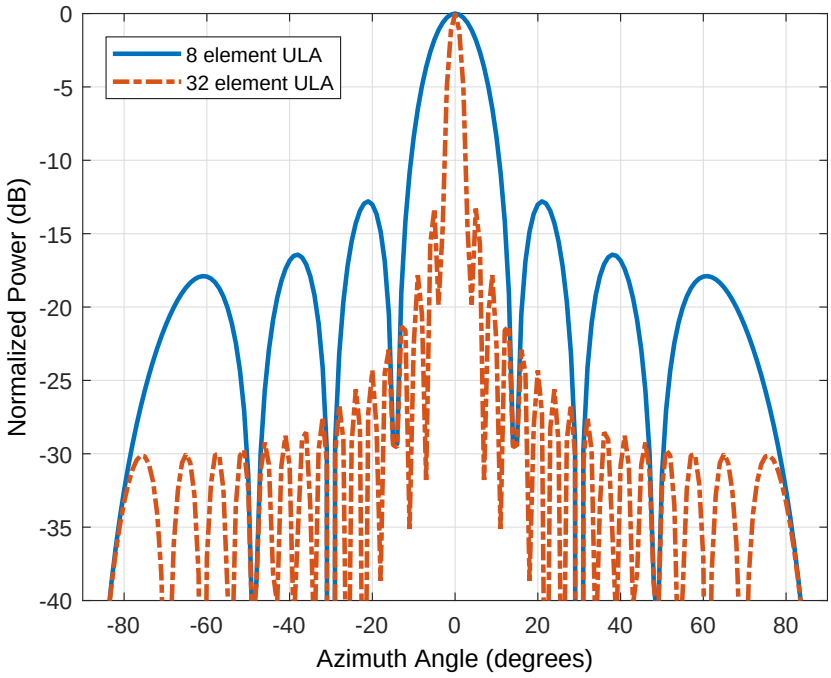

Figure 3.4: Comparison of ULA beam patterns

Figure 3.4 illustrates the beam pattern of two ULAs, the first ULA has eight elements and the second ULA has twenty elements. It can be observed that the sum of the lobes, which includes main lobes and side lobes, equals to the total number of transmit antennas less one. Therefore an antenna array with M transmit antennas can provide $\bar{M}$ DOF, where $\bar{M} = M - 1$. It can also be observed that as the number of antennas increases, the beam width of the main lobe decreases, and the number of side lobes increases.

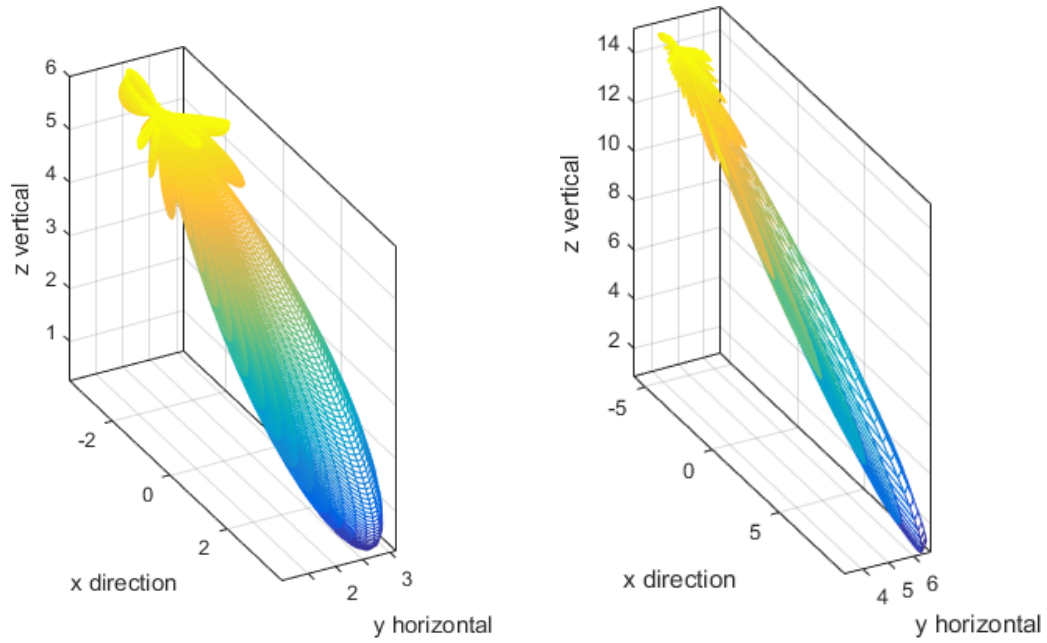

(a) (b)

Figure 3.5: Comparison of 3D beamforming single beams. (a) $\{8 \times 8\}$-URA, and (b)$\{20 \times 20\}$-URA .

Figure 3.5 illustrates 3D beam patterns produced by two URAs. The first URA has 8 elements in the horizontal and 8 elements in the vertical domain. 3D beams give a good idea of how energy is focused when radiated towards the intended UE, where the BS has planar arrays. In order to obtain optimal performance for 3D beamforming in a small cell scenario, the number of array antenna elements should be sufficiently large. It can be observed in Figure 3.5a that the radiation pattern is lower directivity, this is due to the fact that there is a smaller DoF in both the horizontal and elevation domains. It can be observed in Figure 3.5b that the radiation pattern is higher directivity, due to the fact that more energy is within the main lobe when more elements are deployed.

3.6 Summary

This chapter studied and applied the principle of beamforming with antenna arrays to mmWave transmissions. A link budget analysis was given to illustrate the impact of antenna arrays. It showed that as the number of elements increases for a given transmission distance the SE achieved is better, and comparison is based on the single antenna model. The antenna's radiation pattern was investigated to observe how the energy is focused towards a UE. The URA's ability to scan the 3D space was demonstrated. This provides the system model and a general framework for the following chapters.

Chapter 4

TAS as a Knapsack Problem

4.1 Introduction

This chapter introduces the framework of binary Knapsack Problems (KP). A TAS algorithm is developed which satisfies a quality of service (QoS) requirement for a given user. In order to achieve a particular level of QoS, the number of transmit antennas required is determined by remodeling it as a KP. The smallest subset of antenna elements is found at the transmitter side to achieve the desired level of QoS using KP. The KP based TAS algorithm is compared with the low complexity TAS algorithm known as the sequential selection algorithm (SSA).

4.2 TAS mmWave Fundamentals

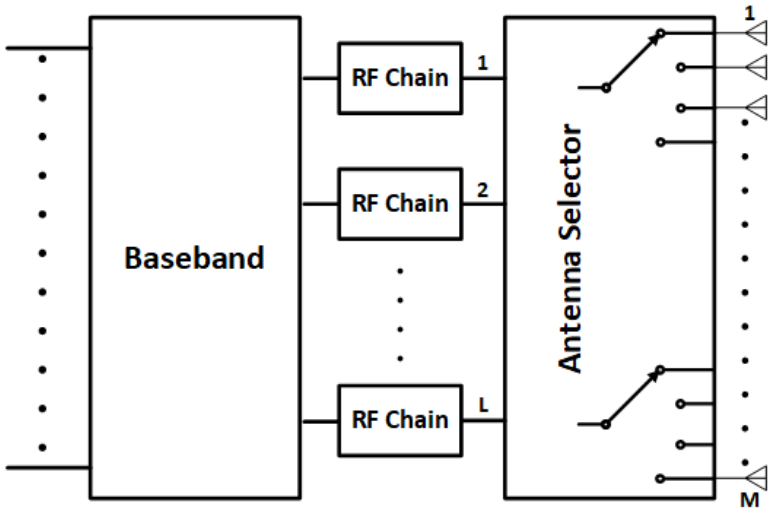

Figure 4.1: Transmit antenna selection

As shown in Figure 4.1, the key feature of antenna selection is that there is a selecting network between L RF chains and M antennas. Based on the channel state information (CSI), the target of antenna selection is to utilize the selecting network to select the best subset of antennas out of the total M antennas for data transmission to maximize the achievable.

The gains of each user's effective channel can be exploited at the transmitter in a TAS based on the acquired CSI. Since mmWave propagation is highly sensitive and vulnerable to obstacles in its path and were investigated in [4, 27, 47, 48]. These works show varying amplitudes across the entire array, demonstrating that all antennas do not contribute equally. However, it can be observed that assigning a smaller number of antennas can be an effective approach to satisfy a given requirement, thus saving power through turning off inactive antennas. Therefore,

transmit antenna selection (TAS) can be employed to reduce system complexity, resulting in an increase SE or EE, since developing effective TAS schemes is critical in mmWave MIMO.

4.2.1 Optimal Transmit Antenna Selection

TAS may be considered as the most classical low RF complexity technology for MIMO systems [83, 84]. TAS schemes tend to select the best M_S elements out of M antennas. However, while this saving tends to come at a small price of performance loss when compared to having all antennas active, if there is a predetermined QoS, there can be a saving in overall power consumption. Optimal TAS can be found through an exhaustive search, however this involves too much complexity as it requires $\binom{M}{M_s}$ combinations and is dependent on the total number of transmit antennas, this becomes impractical especially in the case of massive MIMO. Therefore, low complexity techniques have been proposed which are sub-optimal.

TAS via convex optimization was shown to be optimum in [14, 19], which yields a fractional solution due to the binary relaxation. However, TAS as a KP is a low complex alternative to TAS via convex optimization which avoids the fractional result which requires a further selection of the largest values found. When compared to the low complex solution of sequential selection which is optimum in single user selection, KP can match the performance of SSA. Also it should be noted that KP based selection does not rely on the sorting of the antenna elements which makes it practical for antenna selection in massive MIMO systems.

4.3 Problem Formulation

It is important to determine how many antennas would be required to guarantee a certain QoS. Also, it is required that each transmit antenna selected is assigned to a particular user, therefore a C_k can be achieved between

$$\tilde{C}_k \leq C_k \leq \bar{C}_k, \tag{4.1}$$

where C_k is the required QoS for the kth user, $\tilde{C}_k$ is the minimum QoS and $\bar{C}_k$ is the maximum QoS which is the full array being active. Let $C_k = \alpha_k \bar{C}_k$, where α_k is the threshold value used to achieve a certain level of QoS. The value of α_k varies between $\tilde{C}_k/\bar{C}_k$ and 1, where 1 means that all antenna elements are assigned to the kth user. For $\alpha_k = \tilde{C}_k/\bar{C}_k$, the minimum number of antenna elements are selected for the kth user. For an arbitrary value of α_k, let us suppose M_s antennas are selected, then the capacity will be given by

$$C_k = \log_2\left(1 + \underbrace{\frac{P_k|\boldsymbol{h}_k\bar{\boldsymbol{u}}_k|^2}{M_S\boldsymbol{\sigma}_k^2}}_{q_k}\right), \tag{4.2}$$

where q_k is the SNR requirement of the system. $\bar{\boldsymbol{u}}_k$ is the modified beamforming vector after antenna element selection, given as

$$\bar{\boldsymbol{u}}_k = \boldsymbol{S}_k\boldsymbol{u}_k, \tag{4.3}$$

where $\boldsymbol{S}_k$ represents the selection matrix and is represented as

$$\boldsymbol{S}_k = \mathrm{diag}\left[s_1, s_2, \ldots, s_m\right], \tag{4.4}$$

where

$$s_m = \begin{cases} 1, & \text{if antenna } m\text{th element is selected ,} \\ 0, & \text{otherwise.} \end{cases} \tag{4.5}$$

diag{} performs the diagonal operation forming the diagonal selection matrix. The capacity of the system in terms of received SNR, q_k, can be expressed as:

$$q_k \quad = 2^{C_k} - 1. \tag{4.6}$$

In the proposed adaptive antenna selection technique, the number of active transmitting antennas for mmWave MIMO systems changes adaptively according to the SNR value in the system.

4.4 Transmit Antenna Selection

In order to find the number of transmit antenna elements required, the problem can be represented as

$$\sum_{m=1}^{M} s_m \gamma_m \leq q_k, \tag{4.7}$$

where $\gamma_m = |h_m u_m|^2$ is composed of the channel gain h_m and the beamforming weight u_m is associated with the mth antenna element. γ_m is the m antenna element contribution to SNR and q_k is the QoS requirement. The TAS determines a subset whose total SNR is closest to, without exceeding q_k.

4.4.1 Sequential Selection Algorithm (SSA)

This algorithm uses a sequential selection method to determine the transmit antenna subset [73]. This algorithm sequentially selects antenna elements until the constraint in (4.1) is met. Antenna elements are added, to an empty set, one by one in the order that they appear. SSA can be improved by sorting antennas in a descending order, starting with the best channel conditions to the worst, allowing the best antennas to be combined satisfying the QoS. However, sorting when M is large is quite complex.

Algorithm 1 Algorithm for SSA

Input: M, $\boldsymbol{\gamma}$, q
Output: out
Initialisation :
$s = \text{zeros}(1 \text{ to } M)$
$i = 0$
$j = 0$
for $m = 1$ to M **do**
  $i = i + \gamma[m]$
  if $(i \leq q)$ **then**
    $s[m] = 1$;
    $j = i$
  end if$(i \geq q)$
end for
return s j

4.5 TAS Knapsack Problem

4.5.1 Standard Knapsack Problem

The classical binary KP [77], consists of packing a subset n of N given items into a knapsack of capacity constraint c. Each item has an associated profit and a weight.

$$\begin{aligned} \text{maximize} \quad & \sum_{m=1}^{M} p_j \bar{x}_j \\ \text{subject to} \quad & \sum_{m=1}^{M} w_j \bar{x}_j \leq c, \\ & \bar{x}_j = 0 \text{ or } 1, \quad j \in J = \{1, \ldots, j\} \end{aligned} \tag{4.8}$$

A variation of this problem is to minimize (instead of maximize) the profit summation, under the constraint that the total weight is greater than or equal to a given value.

4.5.2 TAS Knapsack Problem

TAS problems can be efficiently solved as a knapsack problem. The capacity of the knapsack can be regarded as the rate or transmit power requirement and the item types as the antenna contributions to which this resource can be allocated. In our problem the objective of using binary KP is to select the minimal number of antennas which exactly fills the knapsack and maximizes capacity.

TAS KP Algorithm

The optimal $\boldsymbol{S}_k$ can be found by an exhaustive search over all possible combinations which is impractical for mmWave MIMO, due to the extremely large number of combinations [54]. Binary KP can select the minimal number of antennas which exactly fills the knapsack satisfying QoS. The TAS problem is now reformulated

following the the structure of the KP defined in (4.8). The number of selected antennas depends on the QoS required at a UE, which in our case is the user's rate. s_m is the binary decision variable, when $s_m = 1$ the m-th antenna element is selected, and $s_m = 0$ otherwise. In order to find the minimum number of transmit antenna elements required, (4.7) is reformulated as

$$\begin{aligned} \text{maximize} \quad & \sum_{m=1}^{M} \gamma_m s_m \\ \text{subject to} \quad & \sum_{m=1}^{M} \gamma_m s_m \leq q_k, \\ & s_m = 0 \text{ or } 1, \quad m \in M = \{1, \ldots, m\} \end{aligned} \tag{4.9}$$

Our Problem (4.9), is a special case of binary KP with equal values and weights, known as the value independent knapsack problem which is equivalent to the subset sum problem [77]. A general description of the TAS algorithm is described as follows.

Algorithm 2 Algorithm for TAS KP

Input: M, $\boldsymbol{\gamma}$, q
Output: out
Initialisation :
$Q[M+1][q+1]$;
for $m = 0$ to M **do**
  for $n = 0$ to q **do**
    if $(m = 0$ or $n = 0)$ **then**
      $Q[m][n] = 0$;
    else if $(\gamma[i-1] < r)$ **then**
      $Q[m][n] = \max([m-1] + Q[m-1][n - \gamma[m-1]], Q[m-1][n]))$
    else
      $Q[m][n] = Q[m-1][n]$
    end if$(i \geq Q)$
    $n = n + 1$
  end for
  $m = m + 1$
end for
return $Q[M][q]$

4.5.3 Basic Power Consumption Model

Power consumption is important for characterizing the performance of a TAS system. Now we describe an approximated power consumption model for the architecture in Fig. 4.5. A separate RF chain is needed for every active antenna in practical systems, $L = M$. The total power consumed at the BS is given by

$$P_{\text{tot}} = P_{\text{data}} + M_{\text{RF}}(P_{\text{RF}} + P_{\text{ps}}), \tag{4.10}$$

where P_{data} is the total power consumed to transmit the signal. M_{RF} represents the number of active RF chains. P_{RF} is the power consumed by an RF chain. P_{ps} is the power consumed by the phase shifters. From [85], practical values for small cell transmission are considered, since mmWave is more likely to be applied in small cells. Therefore, $P_{\text{data}} = 1\text{W}$, $P_{\text{RF}} = 250\text{mW}$ and $P_{\text{ps}} = 1\text{mW}$. The energy efficiency is given as the capacity divided by the total power consumed, and can be written as

$$\eta = \frac{C}{P_{\text{tot}}}, \tag{4.11}$$

where C denotes the capacity of the system and P_{tot} is the total power consumed which is given in (4.10).

4.5.4 Complexity Analysis

This section provides the complexity evaluation of the transmit antenna selection algorithms. TAS algorithms select a subset of antennas, M_s, from the total number of transmit antennas, M. The complexity is evaluated in terms of the required numbers of multiplications and additions, and is dependent on the number of antennas selected on the BS array.

Table 4.1: Complexity Summary

Algorithm Complexity		
Algorithm	Additions	Multiplications
SSA - unsorted	$4M_s - 2$	$2M_s^2 + 2M_s$
SSA - sorted	$M^2 + 4M_s - 2$	$M^2 + 2M_s^2 + 2M_s$
KP	$4M_s - 2$	$2M_s^2 + 2M_s$

Table 4.1 summarizes and provides the complexity comparison of the KP based antenna selection and the SSA algorithm, sorted and unsorted. The proposed KP and the SSA antenna selection algorithms requires $(4M_s - 2)$ additions and $(2M_s^2 + 2M_s)$ multiplications. However, an additional complexity of (M^2) computations is required for the sorting of the antenna elements according to gains.

4.6 Results

This section discusses the simulations for the achievable capacity of the 3D beamforming in a small cell with KP antenna selection. The affect of the threshold is shown with respect to SNR followed by the comparisons of the SSA (sorted and unsorted) with the KP algorithm. It is assumed that the BS randomly selects users, all having similar QoS requirements.

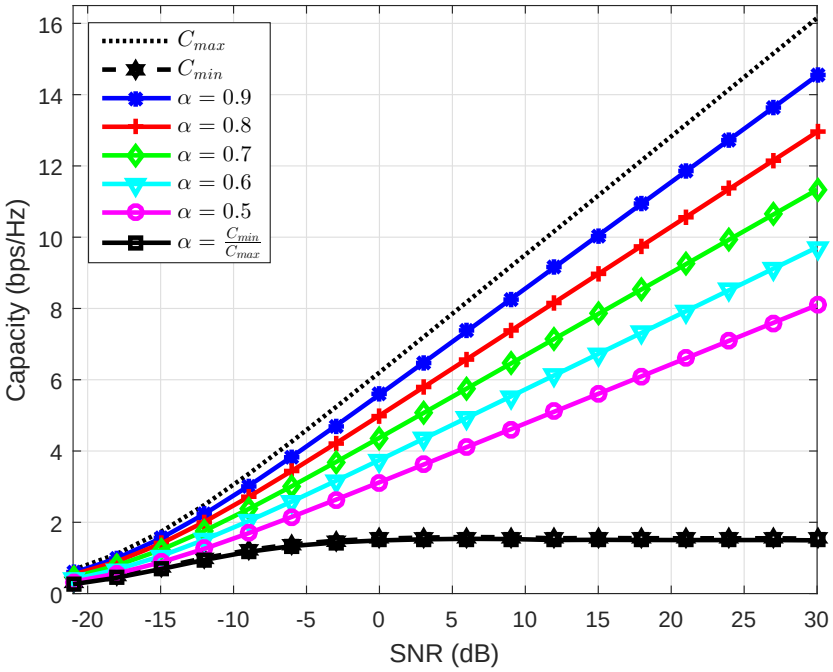

Figure 4.2: The achievable capacity with KP selection based on the QoS requirement in massive MIMO

Figure 4.2 shows the performance of MU-MIMO with 2 users, where the BS has a 10×10 URA and each UE has a single receive antenna. Different values of threshold, α, are compared with SU-MIMO and MU-MIMO. It can be observed that the capacity of MU-MIMO, $C_{\min}$, saturates due to spatial interference. Also the value of α improves from $\alpha = C_{\min}/C_{\max}$, within the range of 0.5 to 0.9, the

capacity of the system improves. Therefore, by using single user performance of a full system as a bench mark, the capacity of the antenna selection using KP can improve overall system performance.

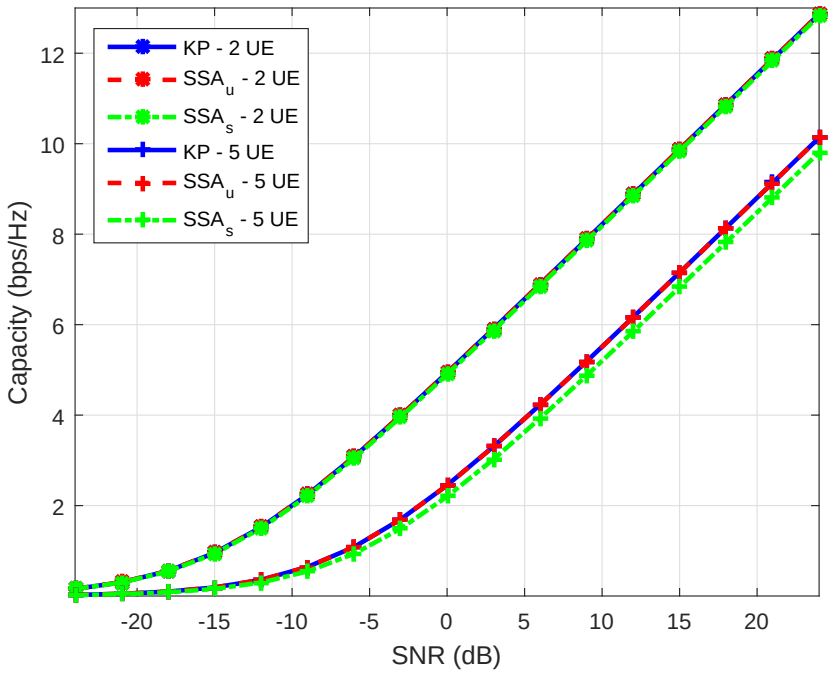

Figure 4.3: The achievable capacity for a reference UE with KP in massive MIMO

Figure 4.3 illustrates the performance of KP in MU-MIMO for a reference user. It can be observed that the capacity of the system improves with the improvement of SNR. However, the capacity decreases with the number of users. From the figure, the performance of KP is similar to that of the SSA_u and SSA_s for the unsorted SSA and sorted SSA respectively. SSA_u performance is better than the SSA_s due to not being sorted.

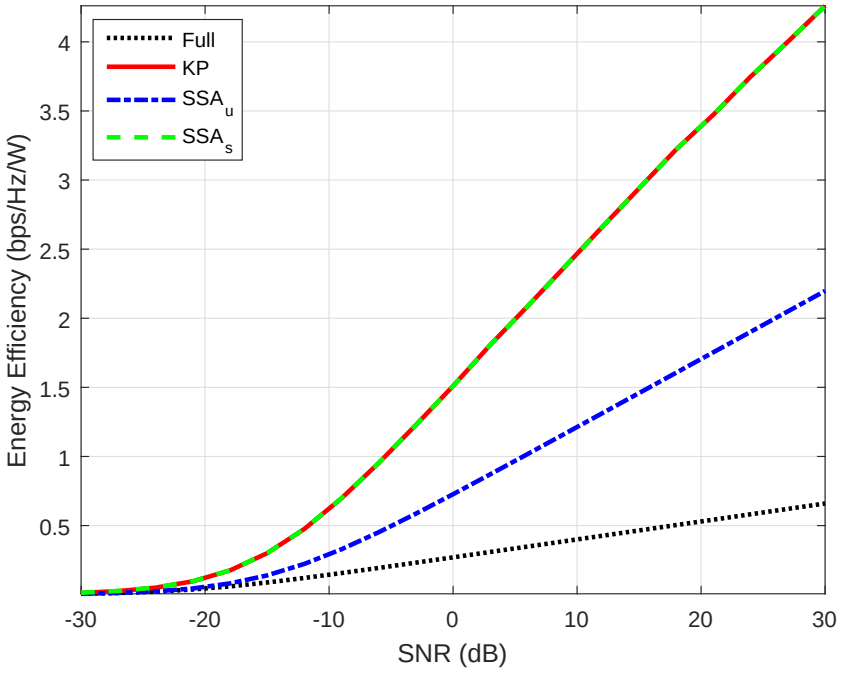

Figure 4.4: The Energy Efficiency of TAS for massive MIMO

In Figure 4.4, a comparison the energy efficiency of KP with the SSA was done. The effects of the transmit power and the number of selected antennas on the energy efficiency is shown. From the graph it can be observed that the energy efficiency improves as SNR increases. It is observed that KP has equivalent energy efficiency with the SSA_s and is superior to the SSA_u. It can also be observed that TAS algorithms have a greater energy efficiency when compared to using all the transmit antennas. Therefore, the KP has good performance in massive MIMO. These results show that larger antenna subsets decrease the energy efficiency, in the case of the SSA_u.

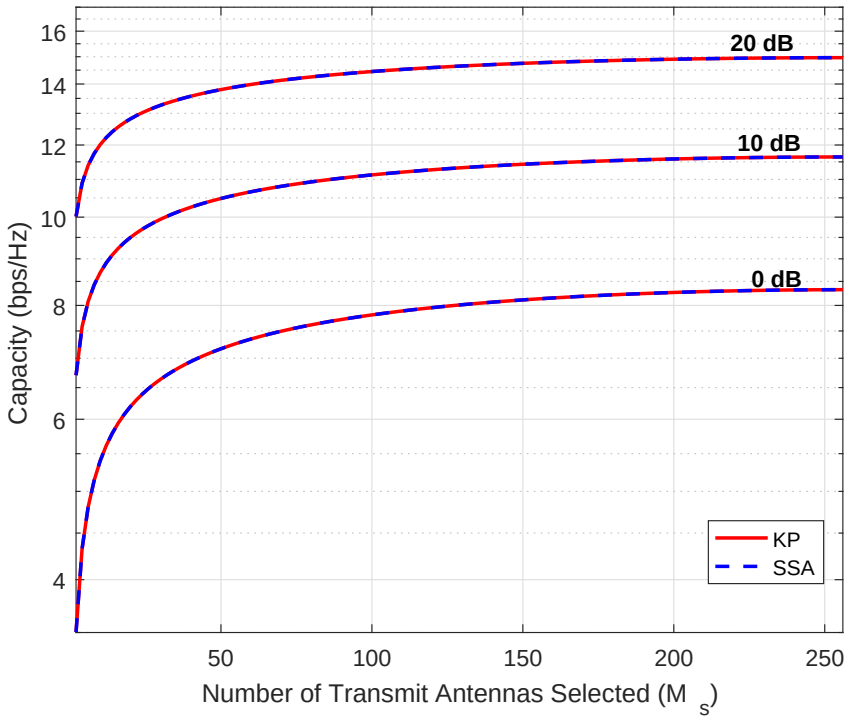

Figure 4.5: The achievable capacity with TAS based on the number of antennas selected (M_s) in massive MIMO

Figure 4.5 shows the performance of SU-MIMO with TAS, where the BS has a 16×16 URA and each UE has a single receive antenna. The figure also shows the capacity performance for different values of SNR, α, as the number of M_s antennas are selected. From the figure it can be observed that the capacity of KP and the SSA are in agreement as the M_s antennas are selected. It can be observed that as M_s increases the capacity of the system improves. However, it can be seen that the KP does not rely on sorting of the elements like the SSA. Therefore, by using single user performance as a bench mark, the capacity of the antenna selection using KP can meet the system requirements, since the SSA finds the local optimum. The single user scenario aims to show the performance of TAS as a binary KP.

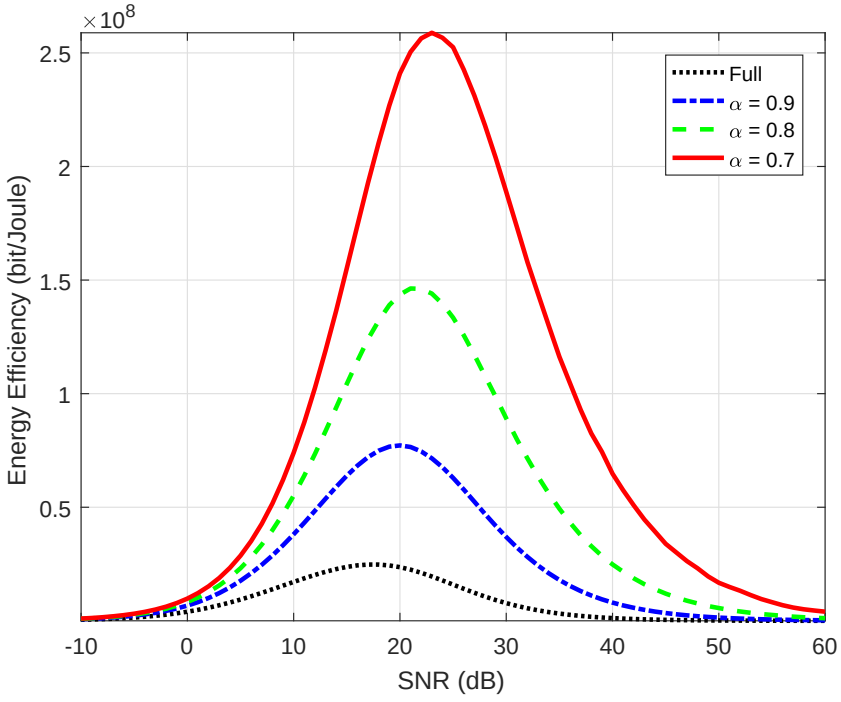

Figure 4.6: The Energy Efficiency with TAS based on a QoS requirement

Figure 4.6 shows the performance of EE for α ranging from 1 to 0.7. The effects of the transmit power and the predetermined QoS requirements on the energy efficiency are shown. It can be observed that at lower QoS requirements there is an increase in EE, this occurs due to more antennas being switched off. Noticeably, at 90% of the full antenna's performance, it can also be observed that there is almost 400% increase in EE around 20dB. However, it can be seen that at high SNR, 50 to 60 dB and low SNR, -10 to 0 dB, the EE are relatively the same. At low SNR with TAS, the difference in α is negligible and the system will require roughly the same number of antennas. It can be observed that as the SNR increases to the high SNR region of 50 to 60 dB, the transmit power dominates the system, although less antennas are required to satisfy QoS.

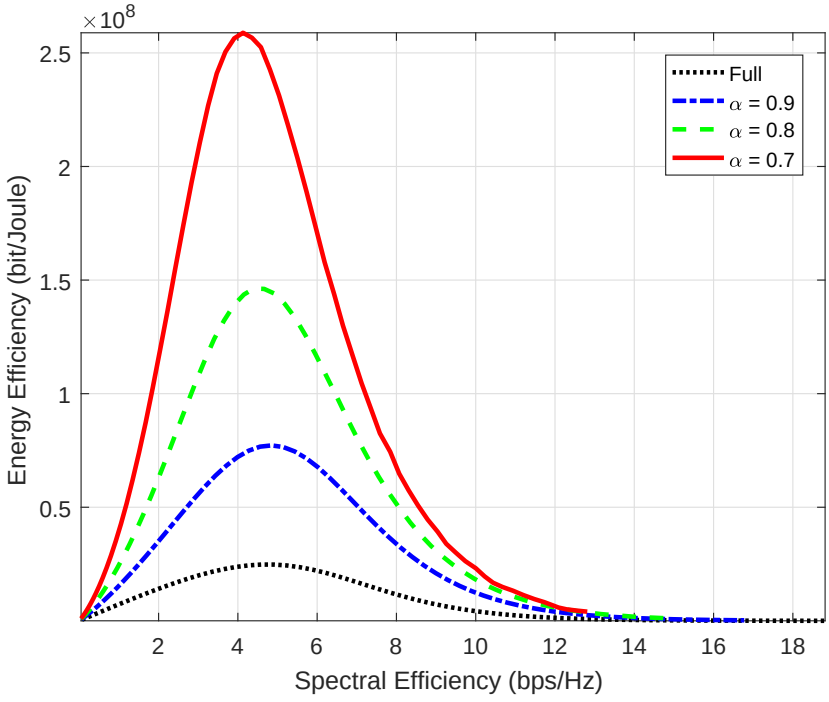

Figure 4.7: The EE and SE trade off for QoS requirements

Figure 4.7 shows the EE and SE trade off for α ranging from 1 to 0.7. It can be observed in Figure 4.7, that $\alpha = 0.7$ a larger EE can be achieved, and when the full array is active or $\alpha = 1$ a larger SE is achieved. However, as the SE increases the EE increases for all values of α until an optimum is reached and then decreases. It can also be observed when $2 < \text{SE} < 7.5$ the maximum EE is achieved when $\alpha = 0.7$. This suggests the further power saving can be achieved for a fixed SE within a certain region. However, for values of $\text{SE} > 7.5$, the EE performance decreases towards that of $\alpha = 1$, and the power savings becomes negligible. The results illustrate that additional power savings can be gained for known QoS requirements.

4.7 Summary

In this chapter the problem of TAS with beamforming for mmWave MIMO was studied with the objective of finding the best antenna subset for a given QoS, showing that EE can be significantly increased which EE is proportional to the number of active transmit antennas. The average rate for a single user was derived for threshold values and compared against the benchmark of the single user with all BS antennas active. A comparison of KP with SSA was shown achieving similar performance, but KP out-performed SSAu in energy efficiency and the computational complexity is lower than the SSAs. TAS is a viable method for reducing overall system complexity.

Chapter 5

Multiuser TAS

5.1 Introduction

In this chapter, a low complexity suboptimal transmit antenna selection algorithm for MU-MIMO systems is proposed. The basic idea of most MU-MIMO approaches is to assign different beams to different users, with baseband digital processing to suppress inter-user interference. The proposed algorithm determines the best subsets of antennas from the total antennas available in the base station for transmission without any special ordering. A comparison of the performance for MU-TAS with conventional MU-MIMO is given. An evaluation of the communication efficiency of TAS is given.

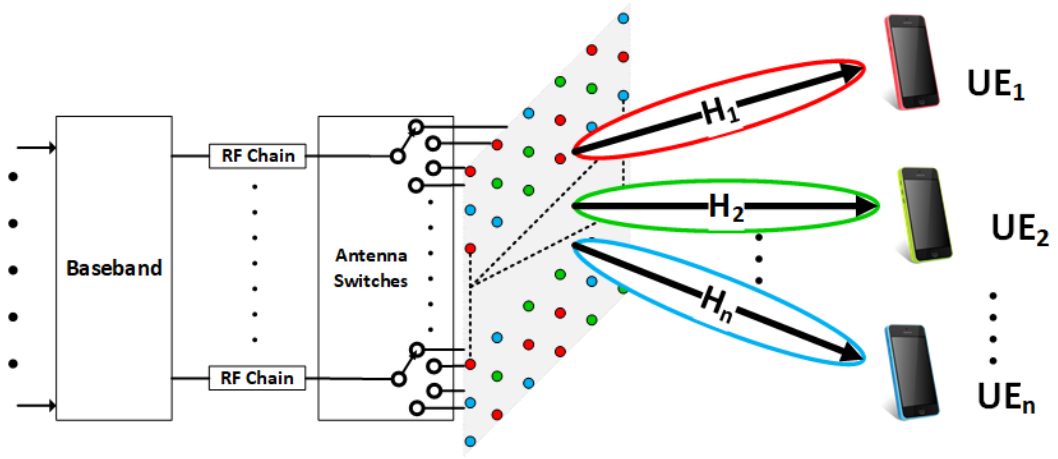

Figure 5.1: Symbolic representation of MU-MIMO with Full Transmit Antenna Array.

5.2 MU-MIMO TAS

Consider the downlink of a 3D-MIMO system as shown in Fig. 5.1. The system consists of a mmWave base station (BS) equipped with M antennas each having a switch, which transmit data to K single antenna user equipments (UEs). The switches indicate that the antennas are being switched on or off for selection. Following the channel model in Chapter 3, the signal model is explained as follows.

5.2.1 Signal Model

The received signal at the kth user is given as

$$y_k = \boldsymbol{h}_k^H \boldsymbol{u}_k \boldsymbol{x}_k + \boldsymbol{h}_k^H \sum_{j \neq k} \boldsymbol{u}_j \boldsymbol{x}_j + \boldsymbol{n}_k, \tag{5.1}$$

where $\boldsymbol{h}_k$ is the channel between the BS and the kth UE, and $\boldsymbol{n}_k$ is the additive white Gaussian noise (AWGN) with zero mean and variance $\boldsymbol{\sigma}^2$. From (5.1), the signal to interference plus noise ratio (SINR) experienced by the kth user is given

as

$$\mu_k = \frac{|\boldsymbol{h}_k^H \boldsymbol{u}_k|^2}{\sum_{j \neq k} |\boldsymbol{h}_k^H \boldsymbol{u}_j|^2 + \boldsymbol{\sigma}_k^2}. \tag{5.2}$$

The achievable rate at the kth user is given by

$$R_k = \log_2(1 + \mu_k). \tag{5.3}$$

The user rate R_k is a nonconvex function with respect to the beamforming vectors u_k.

5.3 Downlink Optimization for Massive MIMO Systems

Massive MIMO systems seek to satisfy a predetermined QoS for a given power constraint. For massive MIMO, the formulation of the downlink beamforming problem is to impose a certain constraint on the received SINR of each user and minimize the total transmit power (or maximize a rate requirement) subject to these constraints. These formulations usually provide the connection to information-theoretical results within the rate region.

5.3.1 Massive MIMO Power Minimization

The power minimization problem of a MU-MIMO downlink under user-specific constraints when the channel vectors are known at the BS, results in an optimization problem and can be written as

$$\begin{aligned} \text{minimize} \quad & \sum_{k=1}^{K} \|\boldsymbol{u}_k\|^2 \\ \text{subject to} \quad & \log_2(1 + \mu_k) \geq \bar{R}_k \end{aligned} \tag{5.4}$$

where $\|\boldsymbol{u}_k\|^2$ is the transmit power to be minimized satisfying a given rate requirement. The problem (5.4) is a convex optimization problem and can be efficiently solved.

5.3.2 Massive MIMO Rate Maximization

When there is a fixed radiated power at the BS for a MU-MIMO downlink channel, the optimization problem can be written as

$$\begin{aligned} \text{maximize} \quad & \sum_{k=1}^{K} \{\log_2(1+\mu_k)\} \\ \text{subject to} \quad & \|\boldsymbol{u}_k\|^2 \leq P_k, \end{aligned} \tag{5.5}$$

where P_k is the transmit power allocated for each UE and solved via convex optimization.

5.4 Problem Formulation

Our problem of interest is to develop a TAS algorithm which can be dynamic and can satisfy the requirements of communication efficiency in a 5G system. The optimal $\boldsymbol{S}_k$ can be found by an exhaustive search over all possible combinations which is impractical for mmWave MIMO, due to the extremely large number of combinations [54]. Therefore it is important to select antennas which satisfy the desired objective. However, it is required that each transmit antenna selected is assigned to one UE only. The objective is to develop a TAS algorithm which maximizes sum-rate of a mmWave system. In a massive MIMO subject to a transmit power constraint, antennas can be chosen such that the number of selected antennas meets a certain transmit power requirement. When there is a fixed radiated power for each UE, at the BS for a MU-MIMO downlink channel, the optimization

problem can be written as

$$\begin{aligned} \text{maximize} \quad & \sum_{k=1}^{K} \log_2 \left(1 + \frac{|\boldsymbol{h}_k^H \boldsymbol{S}_k \boldsymbol{u}_k|^2}{\sum_{j \neq k} |\boldsymbol{h}_k^H \boldsymbol{S}_j \boldsymbol{u}_j|^2 + \boldsymbol{\sigma}_k^2}\right) \\ \text{subject to} \quad & \sum_{m=1}^{M} \boldsymbol{S}_k = M_s \end{aligned} \tag{5.6}$$

$\boldsymbol{S}_k$ is the $M \times M$ diagonal selection matrix of the kth UE and is represented as

$$\boldsymbol{S}_k = \begin{bmatrix} s_1 & 0 & \dots & 0 \\ 0 & s_2 & & 0 \\ \vdots & & \ddots & \vdots \\ 0 & 0 & \dots & s_m \end{bmatrix} \tag{5.7}$$

where

$$s_m = \begin{cases} 1, & \text{if antenna } m\text{th element is selected ,} \\ 0, & \text{otherwise.} \end{cases} \tag{5.8}$$

s variables represent the binary entries in the diagonal selection matrix. However, since the variables of s_m are binary, the optimization problem is NP-hard. The optimal $\boldsymbol{S}_k$ can be found by an exhaustive search over all possible combinations which is impractical for massive MIMO, due to the large number of combinations [14]. TAS via convex optimization yields a fractional solution and is not suitable as it can lead to an antenna being assigned to multiple UEs. Therefore low complexity techniques are of significant interest.

5.5 Low Complexity Transmit Antenna Selection

There is no efficient method to find the global optimal solution at present. In this chapter, the problem is addressed in a sub-optimal but low-complexity way. It is

common practice to reformulate the TAS problem in terms of the SINRs which is equivalent to (5.3) due to the one-to-one monotonic relationship between R_k and μ_k. This relationship makes it possible for TAS algorithms to select transmit antennas based on the channel gains on a per antenna element basis. Therefore it is possible to select K subsets containing M_s transmit antenna elements having the highest powers. This method of TAS is known as the SNR maximization antenna selection and a brief description is given in the following.

SNR Maximization Antenna Selection

This TAS criterion is based on each antenna element's contribution to SNR. The approach is a simple selection process which aims to identify the subset of antennas with the highest contributions to SNR with a sub-optimal approach [86]. The problem is given as follows

$$\mathcal{M} = \max_{M_s}\{\gamma_1, \gamma_2, \cdots, \gamma_m\} \tag{5.9}$$

where $\max_{M_s}$ identifies the M_s highest values, $\mathcal{M}$ is the antenna index subset determined by selection, and M_s is the subset size. $\gamma_m = |h_m u_m|^2$ is composed of the channel gain h_m and the beamforming weight u_m associated with the mth antenna element. Now, using only the contribution to SNR per antenna element as the criteria for selection the problem can be represented as

$$\bar{\mu}_k = \sum_{m=1}^{M} \gamma_{k,m} s_{k,m}, \tag{5.10}$$

where $\bar{\mu}$ is the resultant SNR after TAS is performed. Therefore, it is important to select antennas which maximize the SNR for a predefined subset. Also, it is required that each transmit antenna selected is assigned to one UE.

SNR Matching Antenna Selection

Now, using only the contribution to SNR per antenna element as the criteria for selection the problem can be represented as

$$\sum_{m=1}^{\mathcal{M}} s_{k,m}\gamma_{k,m} \geq q_k, \tag{5.11}$$

where γ_m is the mth antenna element contribution to SNR and q_k is the SINR requirement. The TAS determines a subset whose total SNR is closest to q_k and can be determinded by

$$q_k \quad = 2^{R_k} - 1. \tag{5.12}$$

5.5.1 Multiuser Sequential Selection Algorithm

Following the algorithm provided for SSA to determine the transmit antenna subset, this section extends the SSA to the MU scenario. Now, antenna elements are sequentially selected until the constraint in (5.10) or (5.11) is met. Starting with an empty set, antenna elements are added one by one in the order that they appear. SSA is improved by sorting antennas according to their channel conditions in a descending order, starting with the best to the worst, allowing the best antennas to be combined. One condition of extending the sequential selection method to MU systems for determining the transmit antenna subset, the SSA is restricted to satisfying one UE at a time. Therefore, antenna elements are selected locally by each user based on the selection criteria. Starting with one user at a time, TAS is performed based on the requirements. Once an antenna is selected it is removed from the available set and cannot be reassigned to any other UEs.

5.5.2 Multiple Knapsack Problem Algorithm

Considering the MU-MIMO scenario, each antenna element's SNR contribution varies according to each user. Therefore, the TAS problem can be formulated in the form of a Multiple KP and given a set of transmit antennas M_T and a set of K UEs, each with M_T channel gains. The aim is to select K disjoint subsets of antennas so that the total rate of the system is maximum and each subset contains M_s transmit antenna elements and is assigned to the selected UE. In this case, the sum-rate maximization problem can be formulated as follows

$$\begin{aligned} \text{maximize} \quad & \sum_{k=1}^{K} \sum_{m=1}^{M} \gamma_{m,k} s_{m,k} \\ \text{subject to} \quad & \sum_{m=1}^{M} s_{m,k} \leq M_s, m \in M = \{1, \ldots, m\} \\ & \sum_{k=1}^{K} s_{m,k} \leq 1, \quad k \in K = \{1, \ldots, k\} \\ & s_{mk} = 0 \text{ or } 1, \quad m \in M, \quad k \in K, \end{aligned} \tag{5.13}$$

To find the solution, the problem is solved as binary knapsack sub-problems, which is known as the multiple knapsack problem [77]. For simplicity, the number of RF chains is equal to the number of antennas for the optimization problem of (5.13).

5.5.3 Variable Decision MKP Algorithm

Considering the binary MU-KP formulated in (5.13) where a comparison of all decisions is made before allocating subsets, since it is solved as binary knapsack sub-problems. Therefore it is possible to reduce the overall complexity of the MU-KP decision making to that of a single knapsack problem similar to that in [79]. However, in order to perform this, the channel gain vectors are stacked and a variable decision making criteria is introduced to the problem. Therefore this problem can be represented as follows

$$\begin{aligned} \text{maximize} \quad & \sum_{n=1}^{N} \bar{\gamma}_n \bar{s}_n \\ \text{subject to} \quad & \sum_{k=1}^{K} s_{n-\bar{n}} + ... + s_n + ... + s_{n+\bar{n}} \leq 1, \\ & \sum_{\bar{n}=1}^{N} a_{k,n} s_n \leq M_s, \ k \in K = \{1, \ldots, k\}, \\ & s_n = 0 \text{ or } 1, \quad n \in N = \{1, \ldots, n\}, \end{aligned} \tag{5.14}$$

$\bar{\gamma}_n$ represents nth element of the composite vector of channel gains for the stacked channel matrix, where $N = KM$. $\bar{n}$ represents the position of each UE corresponding element of M_T positions away. $a_{k,n} = 1$ if it is included in the antenna set of the kth UE associated with its position within the stacked channel gains. The introduction of the variable decision criteria, makes it possible for decisions made at a particular time to be changed at anytime during the selection process which improves the flexibility of the decision making in the multiple KP, resulting in a structure similar to that of a single knapsack. After selection is made in a singular KP form, the channel selections can be recovered through partitioning the composite channel vector by associating the channel gains for each selected UE.

5.6 Interference Suppression in Proposed TAS system

Considering the complexity of implementing interference suppression (IS) and TAS simultaneously, a low complexity method is to allow the BS to perform TAS for all UEs and IS at the end. This method allows the best subsets to be easily found for the MU scenario. A practical and simple approach is to employ zero-forcing (ZF) beamforming (BF) to achieve maximum capacity, nulling interference to other users [71]. In ZF TAS with M_s select transmit antennas, the BF vector, u_k, is generated based on the user's channel, h_k, satisfying the following condition:

$$h_k u_j = 0, \quad \forall \;\; j \neq k \tag{5.15}$$

where $1 \leq k$ and $j \leq K$. The IS vectors are designed to completely cancel interference to others achieving interference free transmission.

In the proposed TAS system, the ZF vector is generated while satisfying (5.15), but the transmitter needs to determine the IS vector for each UE. Since each UE is given a different subset, the BS has to design each IS vector according to the selection matrix S_k. Thus in order to perform IS correctly, the BB generate the channel of the intended UE, considering the channels of the other UEs, $\boldsymbol{H} = [\boldsymbol{h}_1, \cdots, \boldsymbol{h}_K]^T$ where $(\cdot)^T$ denotes the transpose of matrix, and $\boldsymbol{h}_k$ is the $M \times 1$ channel vector for the kth UE. To find the IS vector for the kth UE, the following method is adopted.

Let us partition the channel matrix $\boldsymbol{H}$ for the kth UE of interest as

$$\ddot{\boldsymbol{H}}_k = \boldsymbol{H}_k \boldsymbol{S}_k \tag{5.16}$$

where $\ddot{\boldsymbol{H}}_k$ represents the partitioned channel matrix considering the antennas

selected for the kth UE and the interference directions to the other UEs. The IS vector of interest is given by

$$\ddot{\boldsymbol{u}}_k = \ddot{\boldsymbol{h}}_k^T (\ddot{\boldsymbol{H}}_k \ddot{\boldsymbol{H}}_k^T)^{-1} \tag{5.17}$$

where $\bar{\boldsymbol{u}}_k$ represents the partitioned beamforming vector of the kth UE subset with suppression towards the directions of interference for the unintended UEs. The ZF method is performed on the partitioned channel matrix $\ddot{\boldsymbol{H}}_k$, by taking the pseudo-inverse of $\ddot{\boldsymbol{H}}_k$. Now IS has been performed, the additional vectors can be ignored from within the matrix for all unintended users of that particular partition.

5.7 Power Consumption Model

This section introduces the power consumption model for mmWave MIMO communications. The model considers a wireless communication system, where the BS serves K users at different locations, each receiving an individual stream. In this section, descriptions of the power consumption models for the two different structures are given. The BS is equipped with L RF chains and M tightly-packed antennas. Power consumption is important for characterizing the performance of wireless communications systems. The power consumed to transmit signals for the kth UE is the total power radiated by the antenna array at the BS and can be expressed as

$$P_k = \|\boldsymbol{u}_k x_k\|^2 = \|\boldsymbol{u}_k\|^2. \tag{5.18}$$

The basic circuit model is generally composed of the baseband, the RF chains and the phase shifters. Now an approximated description of the power consumption model for the architecture in Fig. 5.2 is given. L RF chains and L^2M phase

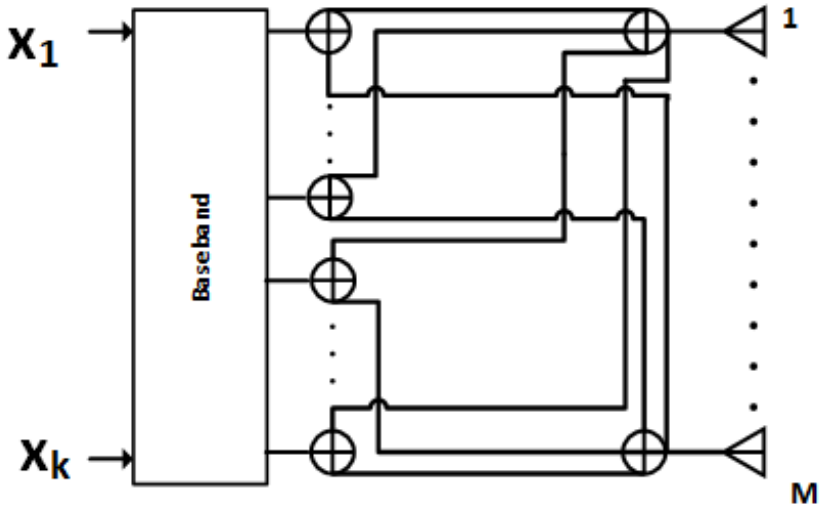

Figure 5.2: Symbolic representation of MU-MIMO with Full Transmit Antenna Array.

shifters are used and the circuit power consumption can be expressed as

$$P_{\text{tot}}^{\text{Full}} = P_{\text{data}} + LP_{\text{RF}} + L^2 M_{\text{RF}} P_{\text{PS}}, \tag{5.19}$$

In Fig. 5.3, L RF chains and M phase shifters are connected. However, when TAS is implemented in a transmission L phase shifters are active, therefore $L = M_{RF}$. The total power consumed at the BS is given by

$$P_{\text{tot}}^{\text{TAS}} = P_{\text{data}} + M_{\text{RF}}(P_{\text{RF}} + P_{\text{PS}}), \tag{5.20}$$

where P_{data} represents the total power consumed to transmit the signal for K UEs. M_{RF} represents the number of active RF chains. P_{RF} is the power consumed by an RF chain. P_{PS} is the power consumed by the phase shifters. From [85], practical values for small cell transmission are considered, since mmWave is more likely to be applied in small cells. Therefore, $P_{\text{data}} = \sum_{k=1}^{K} P_k$, $P_{\text{RF}} = 250\text{mW}$ and $P_{\text{PS}} = 1\text{mW}$. The EE is given as the sum capacity divided by the total power

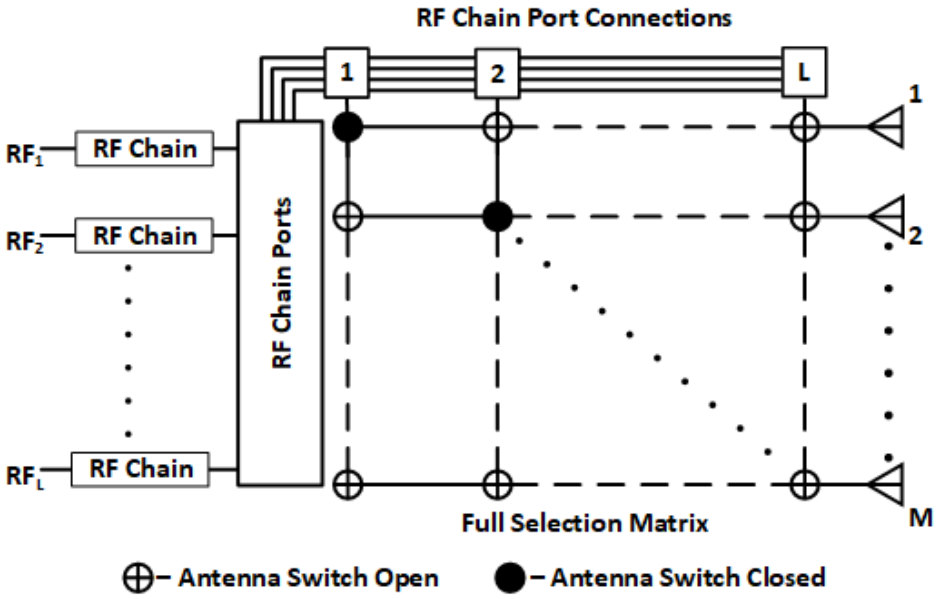

Figure 5.3: Symbolic representation of MU-MIMO with Full Switch Transmit Antenna Selection.

consumed, and can be written as

$$\eta = \frac{C_{\text{sum}}}{P_{\text{tot}}}, \tag{5.21}$$

where $C_{\text{sum}} = \sum_{k=1}^{K} C_k$ denotes the sum capacity of the system and P_{tot} is the total power consumed which is given in (5.19) and (5.20). The capacity can be defined as

$$C_k = B \log_2(1 + \frac{P_L}{N_0 B}\mu) \tag{5.22}$$

where N_0 is the noise power spectral density, B represents the channel bandwidth (in Hertz) and P_L is the power of the distance dependent free space path loss (FSPL).

5.8 Energy Efficiency Gain of TAS Over MIMO

The EE being a ratio between the rate and power, the EE gain between two systems can either be the result of a system providing a better rate than the other system for a fixed transmit power or a lower power consumption for a fixed rate. Therefore the EE gain can be a result of an increase of spectral efficiency (SE) or a decrease in consumed power. For the evaluation of EE gain (G_{EE}) of TAS scheme over full MIMO scheme following [62], the EE gain can is defined as

$$G_{\mathrm{EE}} = \frac{E_{\mathrm{TAS}}}{E_{\mathrm{MIMO}}}. \tag{5.23}$$

Considering an ideal power consumption model, taking into account only the transmit power, the gain is calculated as

$$G_{\mathrm{PCM}} = \frac{P_{\mathrm{MIMO}}}{P_{\mathrm{TAS}}}. \tag{5.24}$$

5.9 Complexity Analysis

In this section, we provide the complexity evaluation of the TAS algorithms. TAS algorithms have to select a subset of antennas, M_s, from the total number of transmit antennas, M and K for the number of selected UEs. The complexity is evaluated in terms of the required numbers of multiplications and additions. The complexity is dependent on the number of antennas in a subset of BS transmit antennas for each UE and the number of UEs in a transmission.

The proposed MKP AS algorithm requires $K(KM + 4M_s - 2)$ number of additions and $K(KM + 2M_s^2 + 2M_s)$ number of multiplications, when K UEs are selected for transmission. Table 5.1provides the complexity comparison of the KP based antenna selection and the SSA algorithm. The proposed VD-MKP and the SSA antenna selection algorithms require $K(KM + 4M_s - 2)$ number of additions

Table 5.1: Multiuser TAS Complexity Summary

Algorithm Complexity		
Algorithm	Additions	Multiplications
Random	$K(4M_s - 2)$	$K(2M_s^2 + 2M_s)$
SSA	$K(KM + 4M_s - 2)$	$K(KM + 2M_s^2 + 2M_s)$
MKP	$K(MM_s + 4M_s - 2)$	$K(MM_s + 2M_s^2 + 2M_s)$
VD-MKP	$K(KM + 4M_s - 2)$	$K(KM + 2M_s^2 + 2M_s)$

and $K(KM + 2M_s^2 + 2M_s)$ number of multiplications. The random antenna selection algorithm requires $K(4M_s - 2)$ number of additions and $K(2M_s^2 + 2M_s)$ number of multiplications. However, an additional complexity of KM computations is required for the sorting of the antenna elements according to gains in the SSA, and for the stacking of the channel gains in the VD-MKP. The MKP requires an additional complexity of KMM_s for the comparison after solving as sub KP problems.

5.10 Low complexity Search Space Reduction Method for TAS systems

Large sets of channel statistics are required in massive MIMO for MU-MIMO, which is based on the total number of antennas and UEs. Therefore it is possible to improve the speed of the decision making of TAS algorithms by employing search space reduction (SSR) techniques. SSR in a TAS system is the removal of the least contributing antenna elements from the overall selection process. Two approaches for SSR are proposed, which are detailed as follows:

Criteria 1 selects the first M_k highest SNR antennas for each UE at the transmitter. This criteria is more practical when a small number of antennas or a small predefined subset size is required, whereas all other elements can be removed from the selection.

Criteria 2 selects antennas above a predefined SNR elemental threshold based on each UE's given rate requirement. Channel gains for each UE at the transmitter can be discarded from the overall set, given that they are the least contributing elements before TAS is performed.

Therefore by employing SSR the subset selections can reach the optimal objective value faster in TAS, since there would be less elements to select overall.

5.11 Results

This section presents the simulation results for the achievable rates when TAS is performed as a binary KP. These simulations are conducted for single user and multi-user scenarios. In the MU scenario the total power P_k for each user is the same. The effect of the number of selected antennas on the sum rate is shown along with comparisons of the random selection, SSA and KP based TAS algorithms. The BS has a 20×20 URA and each UE has a single receive antenna and it is assumed that the BS randomly selects users in a Round Robbin fashion.

Round Robin Selection

Allows the BS to pick a subset of K users to transmit to in a Round Robbin fashion, where at the end of transmitting, all UEs would have received an approximately equal share of transmission time. This scheme requires no feedback information from the UEs to the BS. The average sum-capacity of the Round Robbin scheme is the same for randomly selected users, and it is assumed that the channel state distributions are independent and identically distributed (i.i.d) for all users.

Table 5.2: Simulation Parameters

Simulation Settings	
Carrier Frequency	60 GHz
Spectral Bandwidth	1 GHz
Max radiated power	1 W
Antenna Structure	Planar - URA
Horizontal Elements	20
Vertical Elements	20
Elevation coverage	$-\frac{\pi}{2} \leq \theta \leq \frac{\pi}{2}$
Azimuth coverage	$-\frac{\pi}{2} \leq \phi \leq \frac{\pi}{2}$
BS antenna gain	0 dBi
UE antenna gain	0 dBi
BS antenna height	15m
UE antenna height	ground plane
UE mobility	stationary
Path Loss Model	line-of-sight FSPL
min distance	10m
Cell radius	100m
number of receive antennas	1 (MISO)
number of UEs	1 to 10

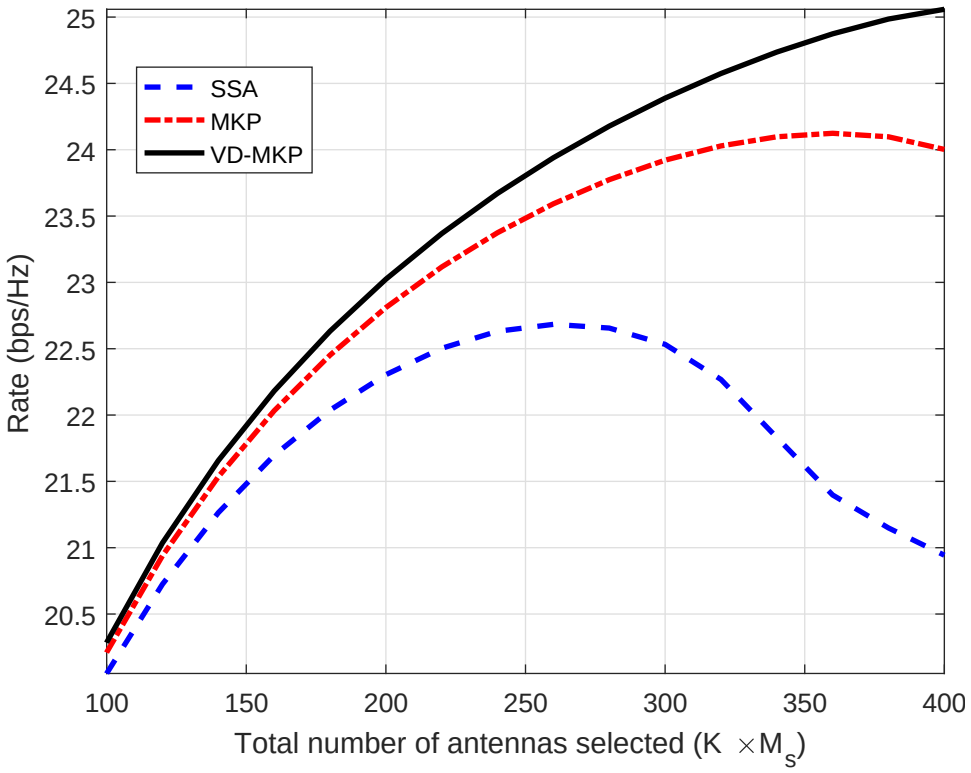

Figure 5.4: Sum-rate of the different antenna selection schemes for an increasing number of BS transmit antennas, $K = 4$, $M_s = 25 : 100$

Figure 5.4 shows the system sum-rate performance versus the number of antennas selected ($K \times M_s$) when SNR = 20dB. From the figure, the proposed algorithms outperform the SSA algorithm. It can be observed that since the SSA is restricted to serving one user at a time the sum-rate is affected by the size of a subset due to one user being served at a time. The SSA can only find the local optimum for any user in the set of available antennas. Therefore for the SSA as M_s increases the number of available antennas is impacted as the best antennas for other users can be removed for other users, which eventually degrades after a maximum is found. Furthermore, as M_s increases, the performance of the VD-MKP algorithm constantly increases and avoids degradation when $K \times M_s > 350$. This means that the proposed algorithm can achieve superior sum-rates. The result shows that for small numbers of M_s the sum-rates achieved are relatively agreeable with all the algorithms. As M_s increases the sum-rate increases till eventually an optimum point is reached then it decreases. Figure 5.4 shows the sum capacity for three UEs against the number of selected transmit antennas M_s in a subset for each UE at different SNR values. It is observed that as M_s also increases the sum capacity increases, and the sum capacity increases with SNR. It can also be seen that TAS as a binary KP achieves a greater sum capacity when compared to the SSA. The SSA is restricted to finding the subset for a single UE at a time. The multiple binary KP does not have that restriction, therefore it can find the subsets which maximize the overall sum capacity.

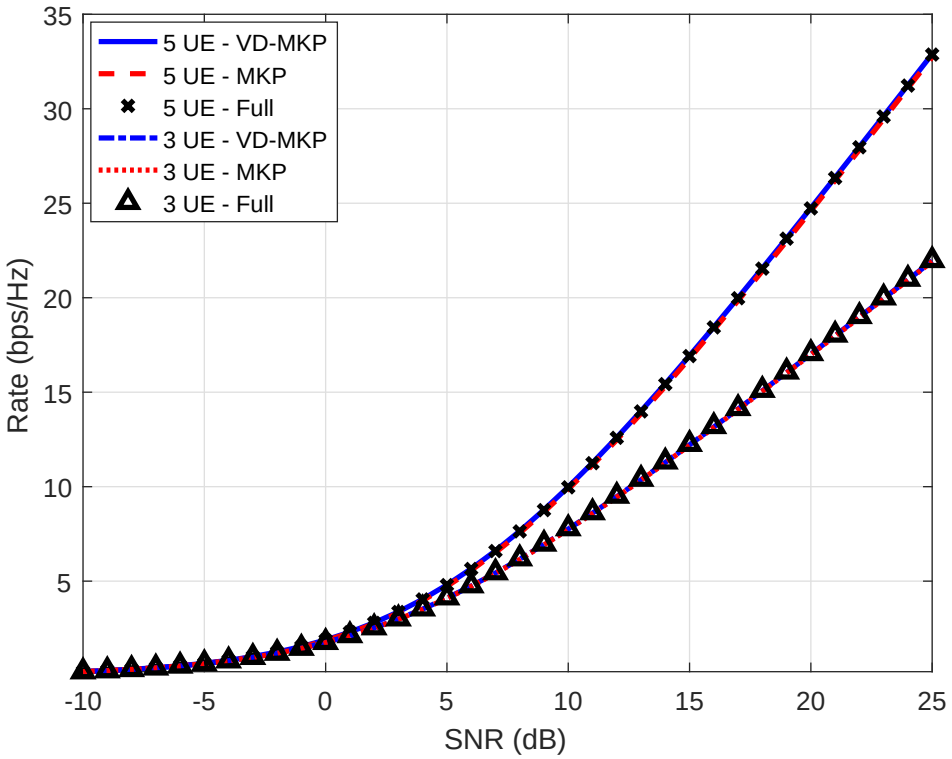

Figure 5.5: The achievable sum capacity with KP based TAS in massive MIMO

Figure 5.5 illustrates the performance of KP in MU-MIMO for three and five selected UEs. It can be observed that the sum capacity of the system improves with the improvement of SNR. However, the sum capacity increases with the number of users. It can be observed that the performance of TAS matches that of all antennas active. Therefore, it shows that it is possible to assign individual subsets per UE and match the achievable sum rate of a full array when all antennas are active.

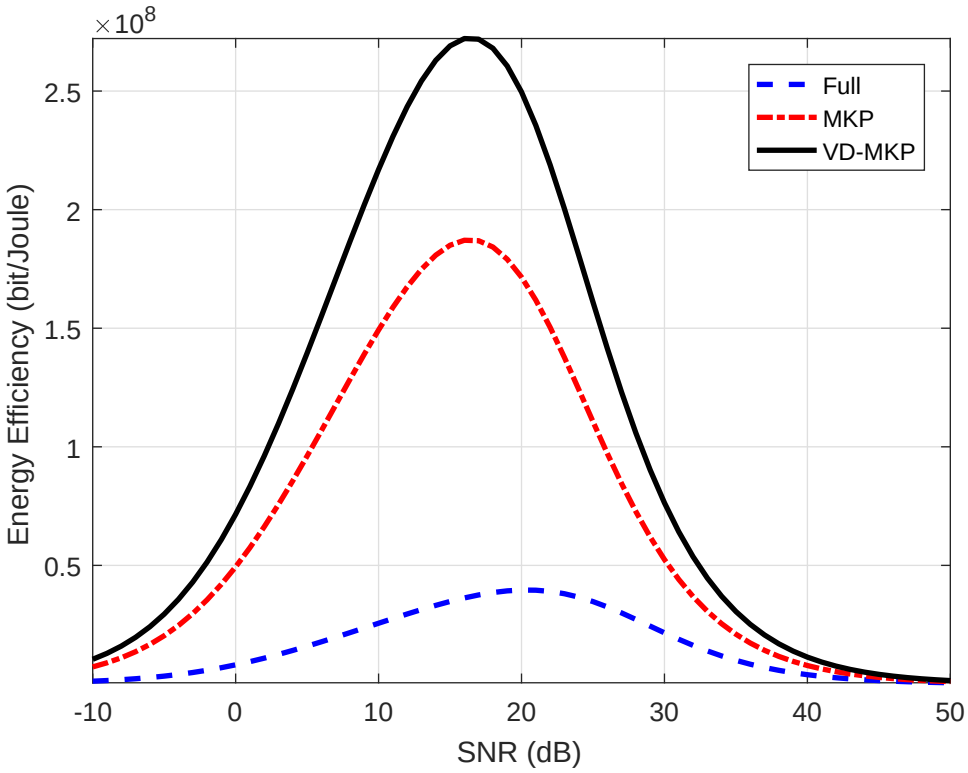

Figure 5.6: The Energy Efficiency of TAS for massive MIMO

Figure 5.6. illustrates the comparison of EE for the TAS algorithms with full array performance in MU-MIMO. From the figure, it can be observed that the EE of the system improves with the increasing of SNR. With conventional methods such as full array, all antennas and associated RF chains are active regardless of transmit power. It can be observed that the performance of VD-MKP has a higher EE than MKP. It can be observed that the TAS algorithms can improve the EE significantly when compared to having all the transmit antennas active. The dashed blue line represents the EE when all the available antennas within the array are active regardless of the transmit power. It can be seen that less antenna elements are required overall by using TAS as when compared to using the full array for transmission. However, it should be noted that the MKP is restricted to solving as knapsack sub-problems, by choosing the best combination of knapsack subsets to maximize SINR, after a pool of possible subsets was created. However, this affects the overall number of elements selected due to the fact that a various number of combinations must be made initially. Therefore, VD-MKP has good performance in massive MIMO systems as it avoids the need to create a pool and select antennas similarly to a single KP with a slight variation. However, it can be observed that TAS algorithms can improve the overall EE significantly in MU-MIMO.

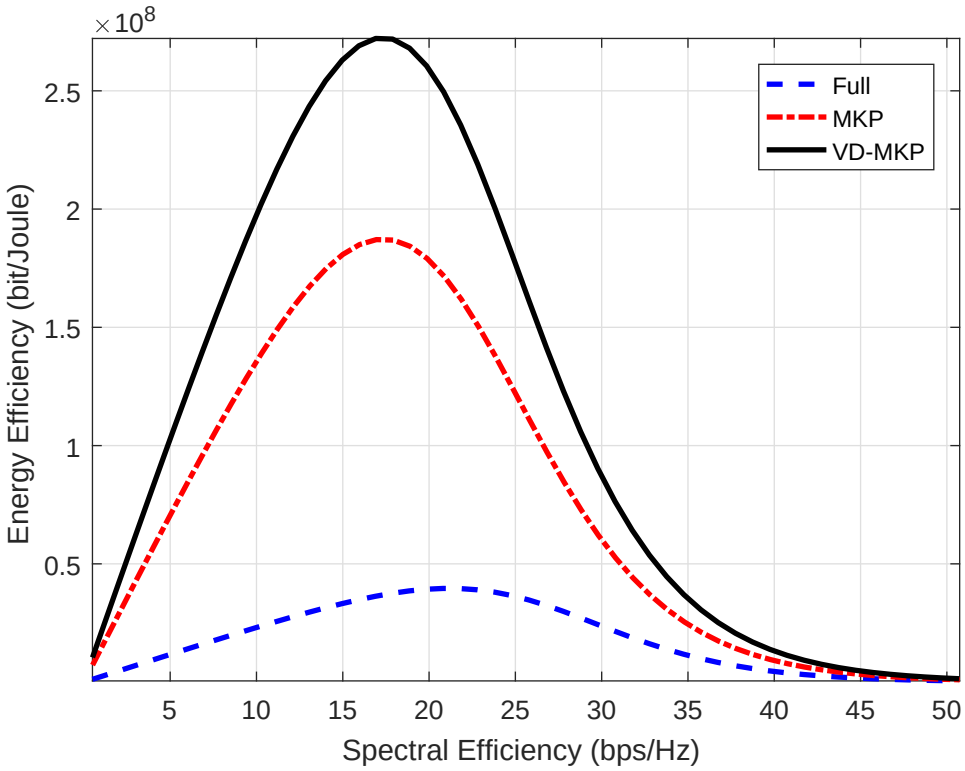

Figure 5.7: Spectral Efficiency vs Energy Efficiency of TAS for massive MIMO

Figure 5.7. illustrates the EE and SE trade-off for the TAS algorithms and the full array schemes in MU-MIMO. It can be seen from Figure 5.7 that the VD-MKP achieves the largest for all cases of SE when $0 \leq SE \leq 50$ bits/s/Hz. The good performance of the TAS schemes can be explained by the fact that the transmit circuit power is dynamically adjusted when antennas are switched on and off to match the required SE. Moreover as the SE increases the number of active antennas required also increases for the TAS schemes. Although the system achieves increased SE, the fixed power consumption due to the transmit circuitry also increases, resulting in a low EE for the full antenna array. In TAS, the circuit power consumption due to the number of active antennas is significantly reduced as antennas are selected to match the SE, which results in increased overall EE when compared to all antennas in the full MIMO array active.

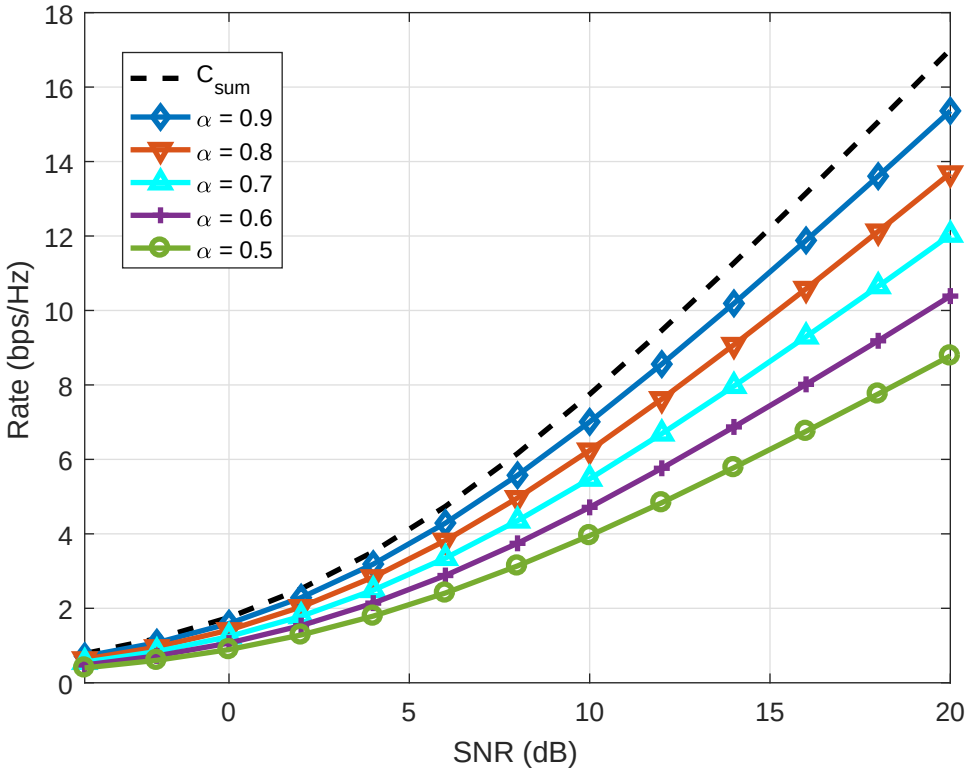

Figure 5.8: The achievable sum capacity with KP in massive MIMO

Figure 5.8. shows the performance of KP in MU-MIMO for three selected UEs. The figure also shows the capacity performance for different thresholds of α and are compared with the full array sum capacity. Considering the transformation in (5.12), a threshold, α, was applied resulting in $\bar{C}_{sum} = \sum_{k=1}^{K} \alpha C_k$. It can be observed that the sum capacity can be matched with KP. Also as the value of α improves within the range of 0.5 to 0.9, the capacity of the system improves. Therefore by using the performance of a full system as a benchmark, the rate achieved by antenna selection using TAS can be varied to satisfy a rate requirement for transmission.

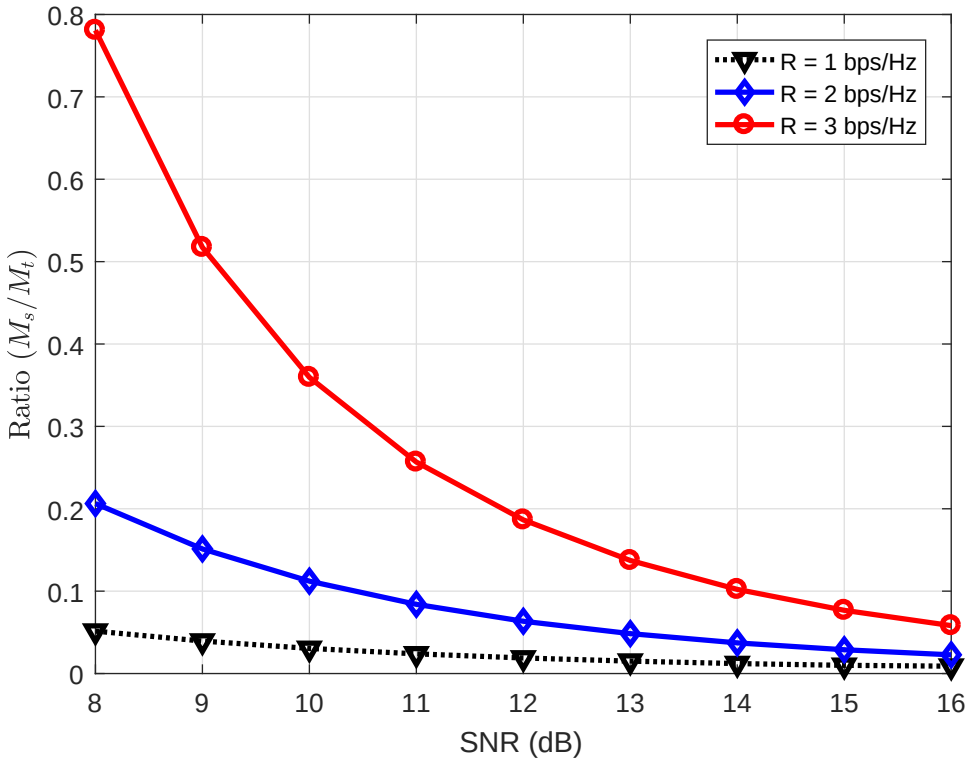

Figure 5.9: The ratio of antennas selected with KP to full antennas in massive MIMO

Figure 5.9. investigates the ratio of number of antennas selected compared to the full set of antennas for fixed rate requirements against the transmit SNR. It can be seen that as the SNR increases, the number of antennas required decreases. However it can also be seen that for higher rate requirements more antennas are required. From this fixed rate analysis it can be observed that more antennas can be switched which will result in a reduced overall power consumption and increased EE. Therefore by employing TAS, a system can be communication efficient for 5G communications.

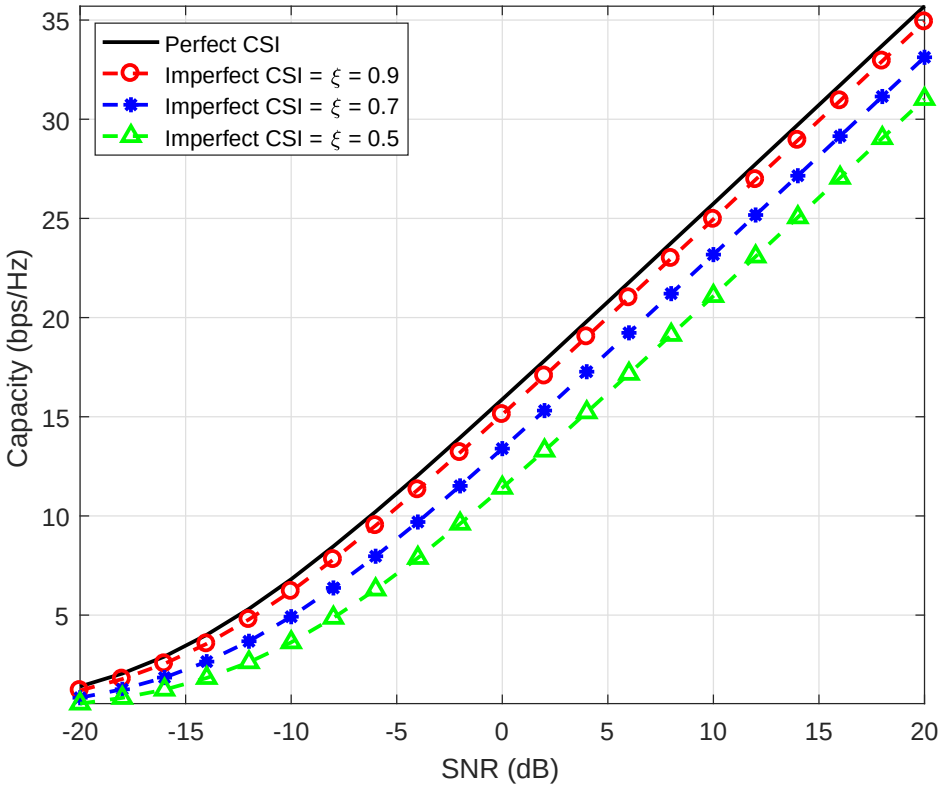

Figure 5.10: The impact of imperfect CSI on sum capacity with KP based TAS in massive MIMO

Figure 5.10 evaluates the impact of imperfect channel state information (CSI) on the proposed KP based TAS algorithm. The estimated channel matrix (imperfect CSI) $\hat{\mathbf{H}}$ can be modeled as [85]

$$\hat{\mathbf{H}} = \xi\mathbf{H} + \sqrt{1-\xi^2}\mathbf{E} \tag{5.25}$$

where $\hat{\boldsymbol{H}}$ is the actual channel matrix, $\xi \in [0, 1]$ presents the CSI accuracy, and $\mathbf{E}$ is the error matrix with entries following the distribution i.i.d. $\mathcal{CN}(0, 1)$. Figure 5.10 shows the achievable rate comparison for KP based TAS in a mmWave system, where the perfect CSI and the imperfect CSI with different ξ scenarios are considered. The effects of imperfect CSI can be observed when $\xi = \{0.9, 0.7, 0.5\}$. The performance of the proposed technique is affected by the errors in the channel estimation. However, it can be observed that when $\xi = 0.9$ the performance is quite close to that of the perfect CSI. Also when the CSI accuracy is quite poor, 80% of the capacity in the perfect CSI scenario can still be achieved.

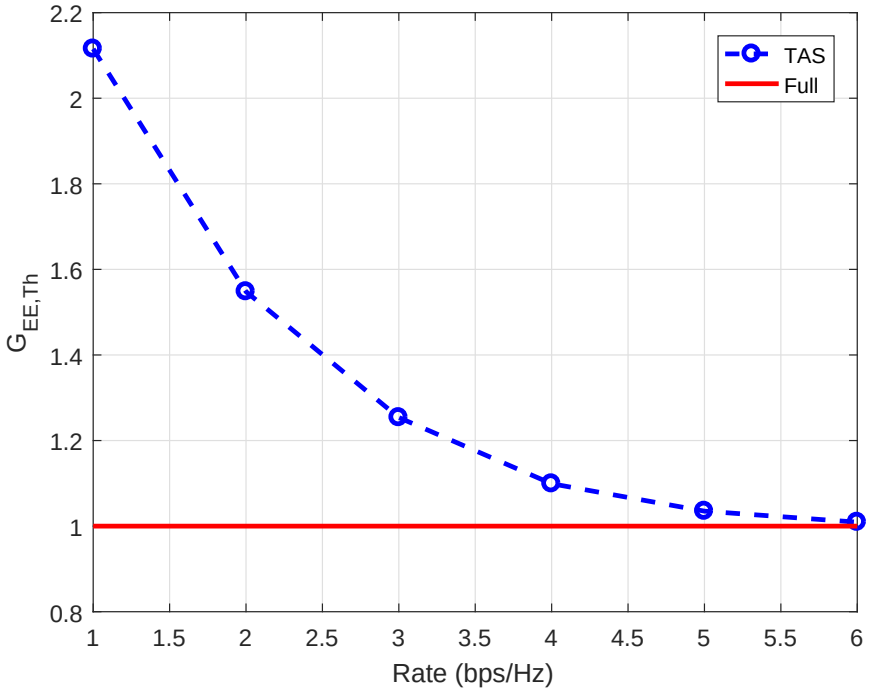

(a)

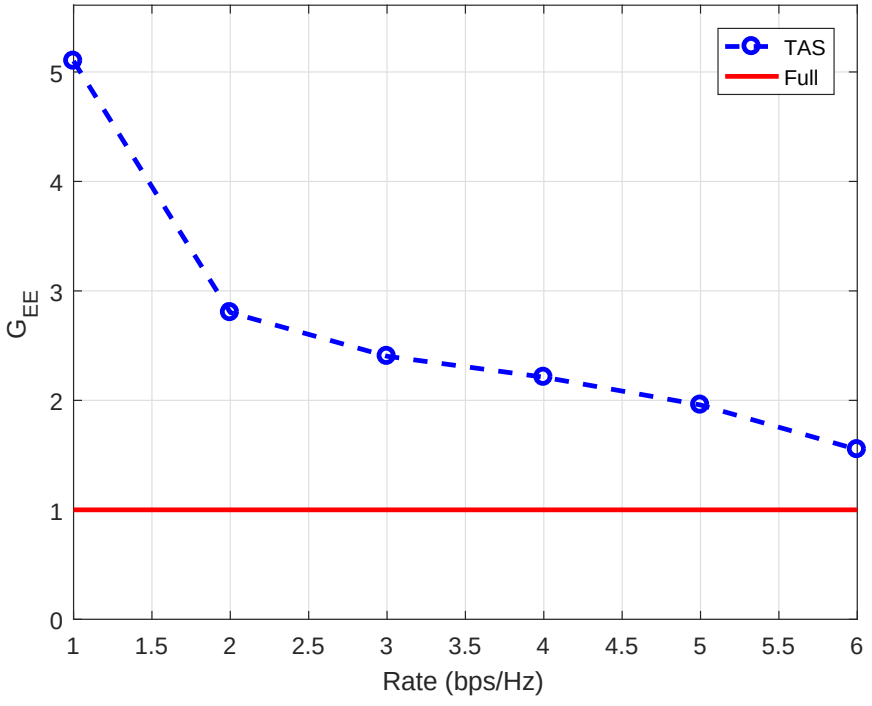

(b)

Figure 5.11: EE gain by using TAS instead of the full array as a function of the Rate. (a) PCM considering P_{data} only. (b) PCM considering P_{tot}.

Figure 5.11 compares the EE gain of TAS scheme over the all antennas active scheme by considering the theoretical power consumption, where only the transmit power is taken into account, and then the power consumption with the power consumed by the RF components. The figure assumes two UEs and illustrates the performance for the gain of TAS, where each UE is given a fixed rate from 1 to 6 bps/Hz. The effect of the transmit power and the number of selected antennas on the EE gain is shown. As expected, the gain decreases as the rate requirement increases in both cases. In Figure 5.11a, it can be seen that TAS is more energy efficient but when P_{data} only is considered in the PCM, the performance gradually approaches that of the full array. However in Figure 5.11b, when the RF circuitry power is considered in the PCM a steady performance gain is maintained between 2 to 6 bps/Hz. This performance gain is maintained due to the fact that the RF power dominates the full array performance as the system approaches its limits.

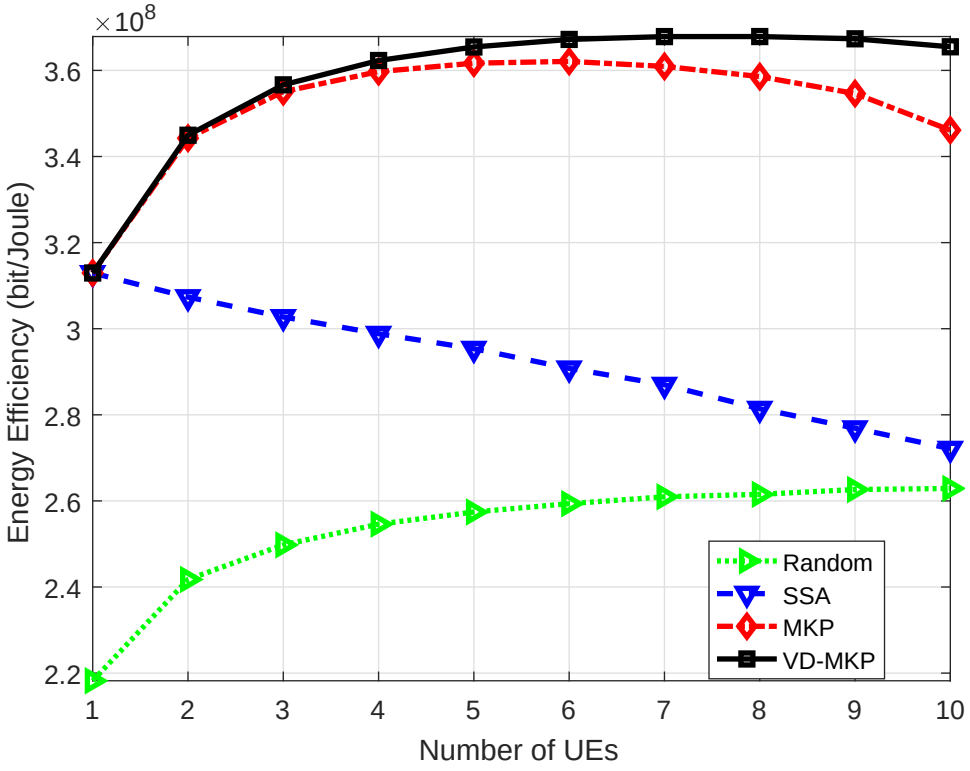

Figure 5.12: Energy-Efficiency of the different antenna selection schemes for an increasing number of active UEs, $M_s = 24$

A plot of the EE for the system as a function of the number of user equipment is given in Figure 5.12. The total initial SNR is set as 5-dB, $M_s = 40$ $M_t = 400$. From Figure 5.12, for a fixed M_s per user the benefits of increasing K in terms of EE eventually saturate, as the number of active antennas eventually dominates the system for a fixed transmit power. It can be seen from the figure that for the SSA the EE decreases linearly due to the fact the sum-rate approaches that of the random selection. Therefore, given the achievable sum-rate and the total power consumption, the energy efficiency of TAS schemes outperforms that of the fully-connected array.

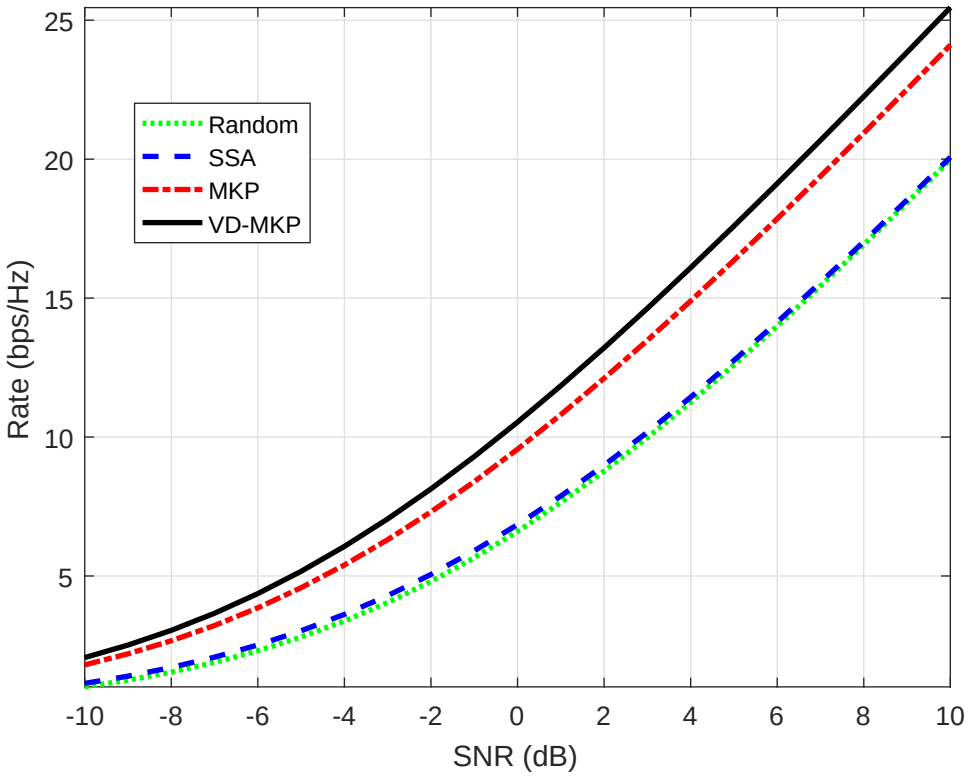

Figure 5.13: Sum Rate of the different antenna selection schemes ($M_s = 80$, $K = 5$ and $M_t = 400$)

In Figure 5.13, the sum rate versus the total initial transmit power is plotted. As shown in Figure 5.13, the sum rate increases with the transmit power. The lowest complexity algorithm random selection is worst performing in terms of sum-rate and the sequential selection offers a better sum-rate. Specifically, the knapsack algorithms provide better performances as expected, by its decision criteria of selecting antennas satisfying each subset requirement but maximizing the overall sum-rate. Moreover, the sum rate of the modified KP outperforms that of the adapted MKP due its flexiblility, which validates the analysis. Furthermore, if all the antennas are selected at the BS as illustrated in Fig. 5.13,it can be observed that the sum-rate performance provided by the proposed algorithms are much higher than that of the SSA and RSA, which verifies the effectiveness of the proposed TAS approaches. The performances of the SSA and RSA are comparable suggesting that the sum-rate of the SSA is directly impacted by the number of antennas in a subset and the total number of available antennas at the BS. It can be seen that the gap between the MKP and the VD-MKP algorithms widens, implying that the VD-MKP is much superior to the MKP and high-quality solution can be achieved.

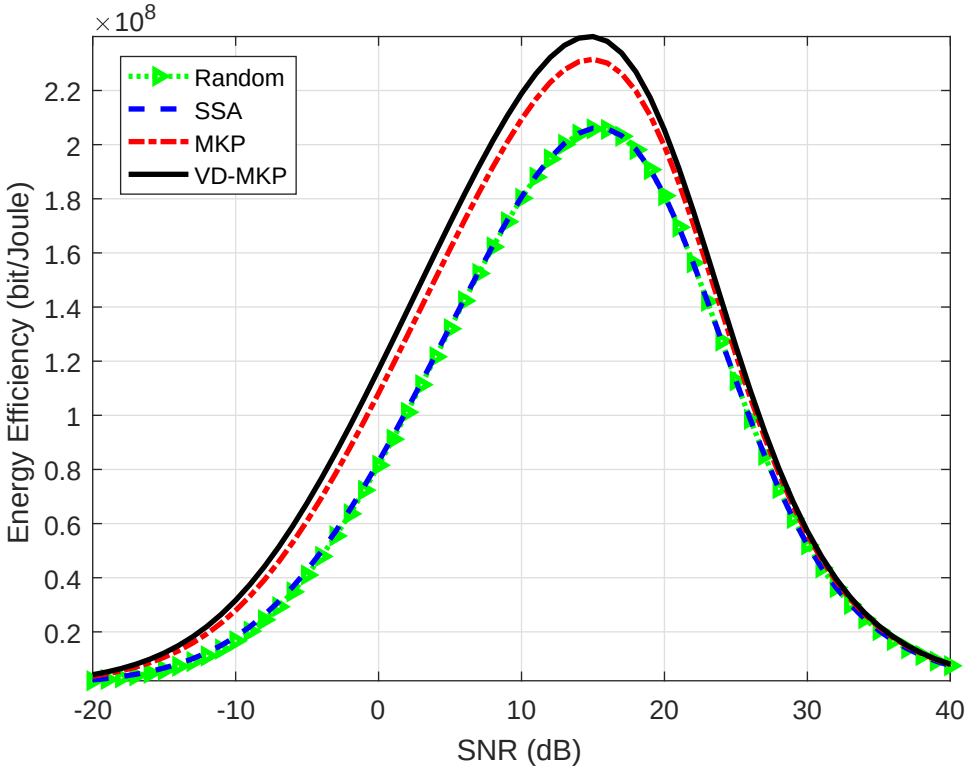

Figure 5.14: Energy-Efficiency of the different antenna selection schemes ($M_s = 80$, $K = 5$ and $M_t = 400$) at 60 GHz

The EE of the different TAS algorithms are illustrated in Fig. 5.14. It can be observed that the EE increases with the transmit power first, then decreases rapidly as the power becomes large. It can be observed that increasing the SNR helps the EE but beyond some point the return is diminishing owing to the logarithmic growth of the systems capacity with power. It can also be observed that the lowest complexity algorithms random selection and SSA have the worst energy efficiencies when all the antennas are split equally among all UEs. Also the VD-MKP has the best EE followed by the MKP, and then the SSA and RSA, respectively.

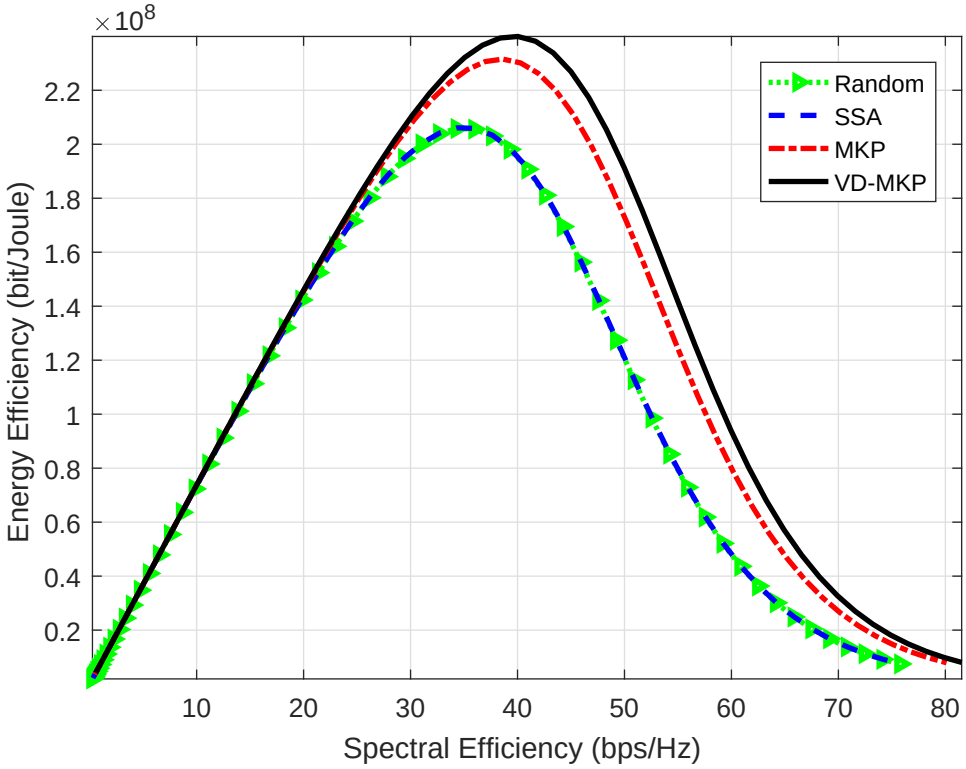

Figure 5.15: Spectral Efficiency versus Energy-Efficiency of the different antenna selection schemes ($M_s = 80$, $K = 5$ and $M_t = 400$) at 60 GHz

Fig. 5.15. demonstrates the system EE versus SE. A discussion of the relationship between EE and SE of TAS algorithms at mmWave frequency of 60 GHz is provided. It can be observed from Fig. 5.15. that, there exists a trade-off between the SE and EE. The figure shows the EE-SE trade-off, indicating the algorithm's optimal performance based on the maximal EE for any given SE. Again, the KP based algorithms have better performances on energy efficiency than the other TAS algorithms. As expected based on the results from Fig. 5.13 and Fig. 5.14, the KP based algorithms achieved a much higher EE for the corresponding SE, considering the SE-EE trade off. It should be noted for the VD-MKP, its peak EE achieved occurred at a SE of 40 bps/Hz, which is largest SE than that any of the other TAS algorithms presented.

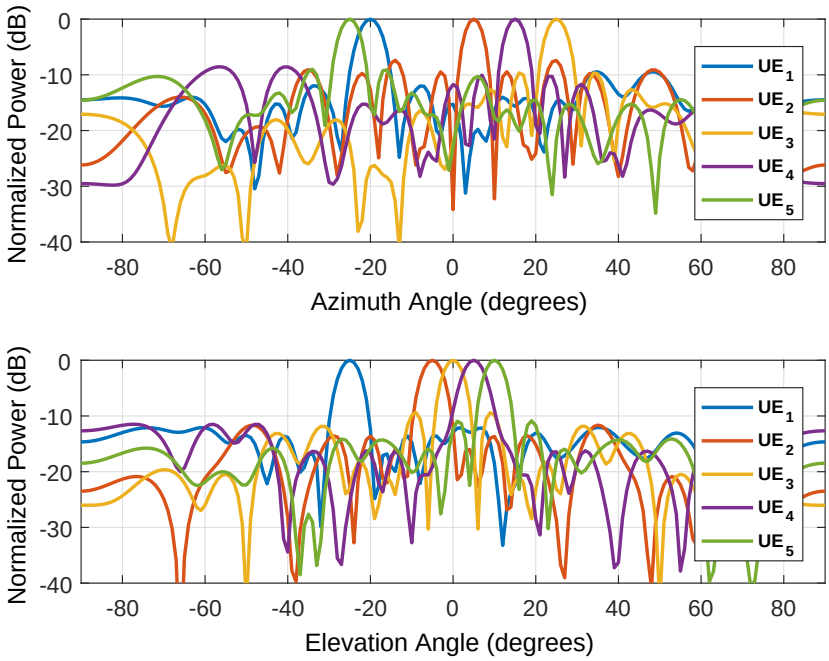

(a) Multi-Beam Pattern without interference cancellation

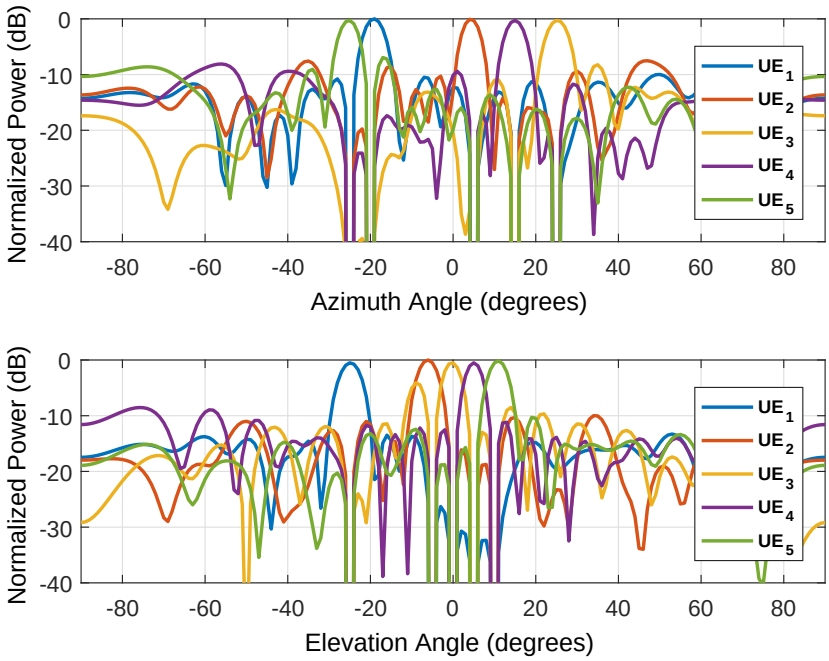

(b) Multi-Beam Pattern with interference cancellation

Figure 5.16: Radiation patterns of MU-MIMO for TAS $M_s = 40$ for $K = 5$

In Figure 5.16, the beampatterns of the BS array serving K-UEs with a set of M_s antennas each are plotted. The number of UEs is fixed to $K = 5$ and $M_s = 40$ for each subset. The azimuth angles of the UEs are $\{-20°, 5°, 25°, 15°, -25°\}$ and the corresponding elevation angles of each UE are $\{-25°, -5°, 0°, 5°, 15°\}$, respectively. However, to make the beam patterns more visually pleasing and easily understandable, Figure 5.16a and Figure 5.16b illustrate the directivity of the main lobes via the azimuth and elevation cuts of the beams respectively after TAS is performed. To showcase the potential of TAS, the beampatterns are plotted when serving 5 UEs with only 40 antennas using standard beamforming (BF) and ZF. Figure 5.16a illustrates the normalized power of TAS-BF, when no IS is preformed. Figure 5.16b. illustrates the normalized power of TAS-ZF when IS performed. It can be observed that TAS algorithms provide good directivity for each user. However in Figure 5.16b, it can be observed that when ZF is performed after TAS, deep nulls are created towards unintended UEs when a main lobe is directed towards a specific UE. These beam patterns are represented as normalised power plots for all values of θ and ϕ, and are useful for visualizing how energy is radiated towards each UE.

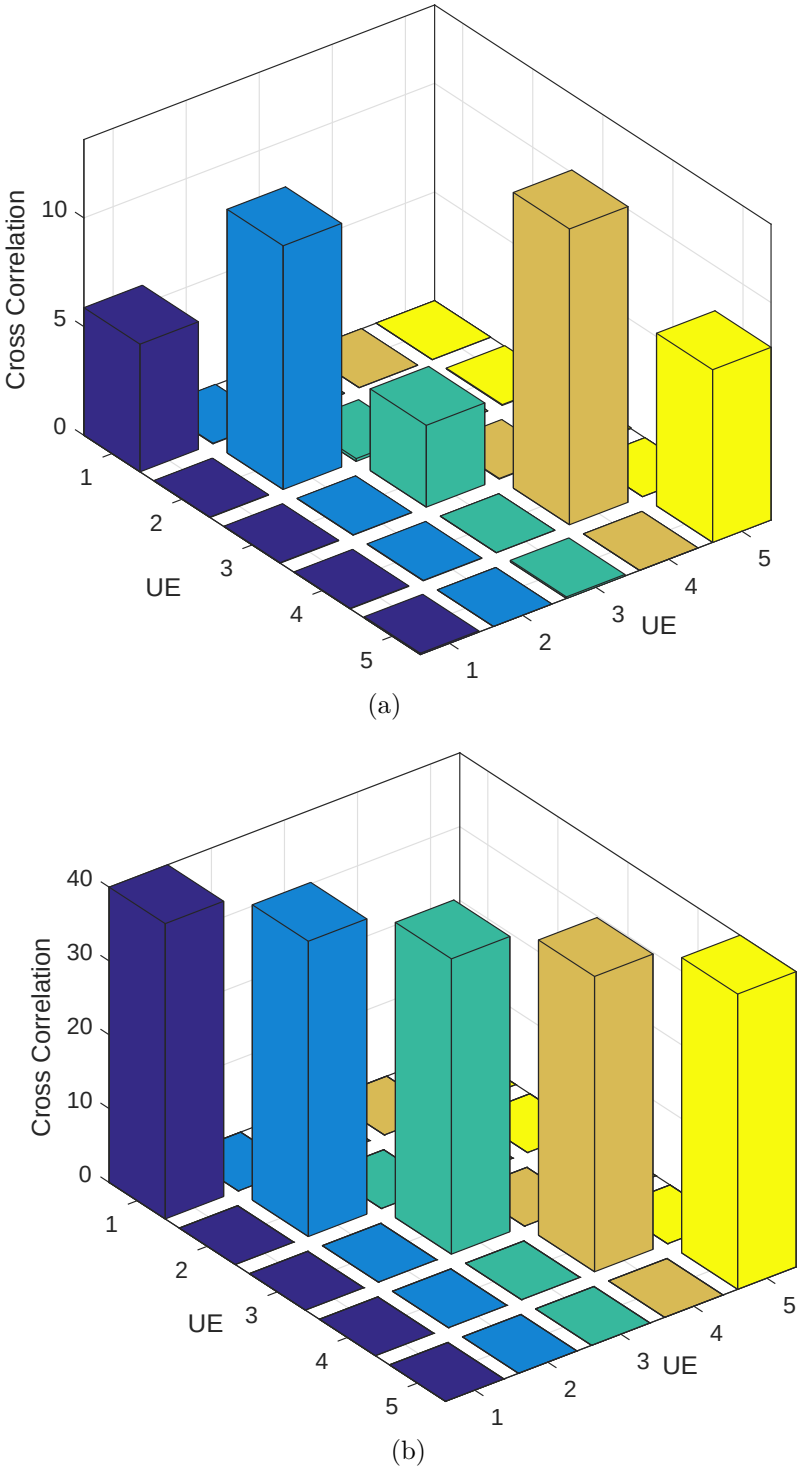

Figure 5.17: Comparison of MU-MIMO for TAS $M_s = 40$ for 5-UE. (a) TAS without interference suppression, and (b) TAS with interference suppression.

Figure 5.17 compares the performance of TAS-BF and TAS-ZF. The figures illustrate the cross-correlation of the radiated energy within each beam towards each UE. The cross-correlation of each beam is a measure of the displacement of energy of the main lobes relative to that of the side lobes of other main lobes within the transmission. It should be noted that TAS-BF is TAS without IS and TAS-ZF is when IS is applied. This analysis considers (5.2) as part of the analysis to help visualize the impact of the received signals of the main lobes and side lobes for K-UEs, when each UE is allocated an equal number of M_s antennas. Given the beam pattern with TAS is a function of

$$G(\theta, \phi) = \left| \sum_{m=1}^{M} s_m \cdot a_m(\theta, \phi) \cdot u_m \right| \tag{5.26}$$

It is now easy to see that the maximum is given by $G(\theta, \phi) = M$ when a beam is directed towards an intended user. However considering that TAS is performed, it is important to inspect this maximum without and with IS, for TAS-BF and TAS-ZF. Therefore when M_s antennas are selected the maximum becomes $G_k(\theta, \phi) = M_s$ for the kth UE, where $M_s = 40$ for these results. Figure 5.17a illustrates the performance of TAS-BF. It can be observed that the maximum gain $G(\theta, \phi) \leq \alpha M_s$ for each UE where $\alpha = 0.25$, this is because the sum of the interfering side lobes significantly impact the main lobes. Figure 5.17b illustrates TAS-ZF, where it can be observed that for any of the main lobes directed towards their intended UEs that the gain is maximum, $G_k(\theta, \phi) = M_s$. It can be seen that IS completely cancels the interference. Therefore by applying TAS with IS, the analysis showed that interference between sub-arrays can be reduced and create multiple beams which can achieve maximum gain that corresponds to the number of antenna elements in a subset.

5.12 Summary

The proposed TAS scheme achieves a similar performance as conventional mmWave MU-MIMO systems. Low complexity schemes are necessary as finding the optimal selection matrix $\boldsymbol{S}_k$ can be carried out by an exhaustive search over all possible combinations. Exhaustive search will be near unachievable for MU-MIMO, due to the extremely large number of combinations, as complexity exponentially scales with K UEs. A noticeable result of TAS is that a significant number of transmit antennas can be switched off for a percentage of the total capacity. Results illustrate that TAS schemes achieve significant gains in communication efficiency. Simulation results show that the proposed algorithm achieves a superior performance compared to other low complexity TAS algorithms.

Chapter 6

Conclusions and Future Works

6.1 Conclusions

In 5G systems, mmWave MIMO is one of the most promising technologies to provide high data rates. Researchers are investigating digital and hybrid beamforming, but such systems are still costly and power hungry due to the large number of RF chains required to connect the antennas to baseband for efficient transmissions, regardless of the configuration. The total power consumption of these architectures poses a problem in 5G systems given the requirement of communication efficiency.

The problem of TAS with beamforming for mmWave MIMO with the objective of finding the best antenna subset for a given QoS was studied, showing that the number of transmit antennas can be significantly reduced. The average rate for a single user was derived for threshold values and compared against the benchmark of the single user with all BS antennas active. A comparison of KP with SSA was shown achieving similar performance, but KP out-performed SSAu in energy efficiency and the computational complexity is lower than the SSAs. TAS is a viable method for reducing overall system complexity, whilst maintaining the QoS with

smaller subsets.

Furthermore, a low complexity design for TAS algorithm was proposed and analyzed for multiuser scenarios in massive MIMO. A knapsack based antenna selection technique for MU-MIMO has been proposed. The design goal of this system was to select antenna subsets per UE which maximizes the total sum rate of the system. The objective of selecting transmit antennas was to find the best subset, given the subset constraints. Comparison was done with variable decision multiple KP (VD-MKP), multiple knapsack (MKP), sequential selection algorithm (SSA) and random selection. It was concluded that the sum rates of the binary KPs are higher than that of the low complexity SSA and random selection. Also the VD-MKP outperformed the MKP in all performance measures. The variable decision criteria of the proposed scheme is more flexible than that of the MKP. Antenna selection is a viable method in reducing overall system complexity in massive MIMO.

This thesis addressed some of the key challenges of communication efficiency for 5G systems with the design of TAS systems for mmWave MIMO. It can be concluded the TAS MIMO provides scalability based on the specific system requirements (i.e. power or rate). Since antenna arrays will be part of any solution in 5G, TAS provides additional simplicity with appliying more classical beamforming techniques, allowing multiuser support and great service to all users. It should be noted that splitting the multiantenna at the base station into subsets does not decrease the performance. User specific beams and data are allowed and propagation is almost always as favorable.

6.2 Future Works

The work in this thesis provides a platform for TAS which find the best subset on a per user basis. This thesis assumed a single cell MU-MIMO downlink mmWave system with single receive antenna UEs. However, this issue can be extended to cover

- The impact of multiple receive antennas at the UE in mmWave MIMO networks. Joint transmit and receive antenna selection can be studied. The EE can be modelled to include the receive power consumption. The will give a full view of the communication link to determine better communication efficiency, especially at the UE as lower power consumption is necessary.
- Further analysis in the search space reduction techniques can be done to more alleviate the complexity of the algorithm as the number of transmit antennas or UEs increase. The preprocessing of the antenna will help to remove the least likely antennas to be selected.

For joint transmit and receive antenna selection, the impact of antenna correlation can be included. Practical antennas signals may be correlated either at the BS and/or the UE. Therefore it is critical to estimate the performance in non-ideal scenarios. Hence, investigating these points for antenna selection in mmWave MIMO, will ensure more communication efficient solutions for 5G wireless systems.

Bibliography

[1] M. Series, "IMT Vision–Framework and overall objectives of the future development of IMT for 2020 and beyond," 2015.

[2] 3GPP, 3rd Generation Partnership Project, "Overview of 3GPP Release 13 V0.0.5 (2014-03)," June 2014.

[3] 3GPP TS 23.501 ver 0.2.0 Release 15, "System architecture for the 5G system," Feb. 2017.

[4] M. R. Akdeniz, Y. Liu, M. K. Samimi, S. Sun, S. Rangan, T. S. Rappaport, and E. Erkip, "Millimeter Wave Channel Modeling and Cellular Capacity Evaluation," *Selected Areas in Communications, IEEE Journal on*, vol. 32, pp. 1164–1179, June 2014.

[5] M.-M. Chiou and J.-F. Kiang, "Attenuation of Millimeter-Wave in a Sand and Dust Storm," *IEEE Geoscience and Remote Sensing Letters*, vol. 13, pp. 1094–1098, Aug. 2016.

[6] Z. Gao, L. Dai, D. Mi, Z. Wang, M. A. Imran, and M. Z. Shakir, "MmWave massive-MIMO-based wireless backhaul for the 5G ultra-dense network," *IEEE Wireless Communications*, vol. 22, pp. 13–21, Oct. 2015.

[7] J. Zhang, X. Ge, Q. Li, M. Guizani, and Y. Zhang, "5G Millimeter-Wave Antenna Array: Design and Challenges," *IEEE Wireless Communications*, vol. PP, no. 99, pp. 2–8, 2017.

[8] Y. Wang, J. Xu, and L. Jiang, "Challenges of System-Level Simulations and Performance Evaluation for 5G Wireless Networks," *IEEE Access*, vol. 2, pp. 1553–1561, 2014.

[9] A. Adhikary and G. Caire, "Joint Spatial Division and MultiplexingâĂŤThe Large-Scale Array Regime," *IEEE Transactions on Information Theory*, vol. 59, pp. 6441–6463, Oct 2013.

[10] X. Peng, W. Wu, J. Sun, and Y. Liu, "Sparsity-Boosted Detection for Large MIMO Systems," *IEEE Communications Letters*, vol. 19, pp. 191–194, feb 2015.

[11] Z. Xiao, X.-G. Xia, D. Jin, and N. Ge, "Iterative Eigenvalue Decomposition and Multipath-Grouping Tx/Rx Joint Beamformings for Millimeter-Wave Communications," *IEEE Transactions on Wireless Communications*, vol. 14, pp. 1595–1607, mar 2015.

[12] H. Zhu, "Performance comparison between distributed antenna and microcellular systems," *IEEE Journal on Selected Areas in Communications*, vol. 29, pp. 1151–1163, June 2011.

[13] T. Alade, H. Zhu, and J. Wang, "Uplink spectral efficiency analysis of in-building distributed antenna systems," *IEEE Transactions on Wireless Communications*, vol. 14, pp. 4063–4074, July 2015.

[14] S. Mahboob, R. Ruby, and V. C. M. Leung, "Transmit antenna selection for downlink transmission in a massively distributed antenna system using convex optimization," in *2012 Seventh International Conference on Broadband, Wireless Computing, Communication and Applications*, pp. 228–233, Nov 2012.

[15] J. Wang, H. Zhu, and N. J. Gomes, "Distributed antenna systems for mobile communications in high speed trains," *IEEE Journal on Selected Areas in Communications*, vol. 30, pp. 675–683, May 2012.

[16] H. Zhu and J. Wang, "Radio resource allocation in multiuser distributed antenna systems," *IEEE Journal on Selected Areas in Communications*, vol. 31, pp. 2058–2066, October 2013.

[17] H. Osman, H. Zhu, D. Toumpakaris, and J. Wang, "Achievable rate evaluation of in-building distributed antenna systems," *IEEE Transactions on Wireless Communications*, vol. 12, pp. 3510–3521, July 2013.

[18] E. G. Larsson, O. Edfors, F. Tufvesson, and T. L. Marzetta, "Massive MIMO for next generation wireless systems," *IEEE Communications Magazine*, vol. 52, pp. 186–195, February 2014.

[19] X. Gao, O. Edfors, F. Tufvesson, and E. G. Larsson, "Massive MIMO in Real Propagation Environments: Do All Antennas Contribute Equally?," *IEEE Transactions on Communications*, vol. 63, pp. 3917–3928, Nov 2015.

[20] S. Rangan, T. S. Rappaport, and E. Erkip, "Millimeter-Wave Cellular Wireless Networks: Potentials and Challenges," *Proceedings of the IEEE*, vol. 102, pp. 366–385, mar 2014.

[21] J. Costantine, Y. Tawk, S. E. Barbin, and C. G. Christodoulou, "Reconfigurable Antennas: Design and Applications," *Proceedings of the IEEE*, vol. 103, pp. 424–437, Mar. 2015.

[22] O. Tervo, L.-N. Tran, and M. Juntti, "Optimal Energy-Efficient Transmit Beamforming for Multi-User MISO Downlink," *IEEE Transactions on Signal Processing*, vol. 63, pp. 5574–5588, Oct. 2015.

[23] J. Zhang, X. Huang, V. Dyadyuk, and Y. Guo, "Massive hybrid antenna array for millimeter-wave cellular communications," *IEEE Wireless Communications*, vol. 22, pp. 79–87, Feb. 2015.

[24] O. El Ayach, S. Rajagopal, S. Abu-Surra, Z. Pi, and R. W. Heath, "Spatially Sparse Precoding in Millimeter Wave MIMO Systems," *IEEE Transactions on Wireless Communications*, vol. 13, pp. 1499–1513, Mar. 2014.

[25] M. Marcus, "Spectrum policy issues for millimeter wave mobile communications [spectrum policy and regulatory issues]," *Wireless Communications, IEEE*, vol. 21, pp. 8–9, December 2014.

[26] M. N. Kulkarni, A. Ghosh, and J. G. Andrews, "A Comparison of MIMO Techniques in Downlink Millimeter Wave Cellular Networks With Hybrid Beamforming," *IEEE Transactions on Communications*, vol. 64, pp. 1952–1967, May 2016.

[27] M. K. Samimi, G. R. MacCartney, S. Sun, and T. S. Rappaport, "28 GHz Millimeter-Wave Ultrawideband Small-Scale Fading Models in Wireless Channels," in *2016 IEEE 83rd Vehicular Technology Conference (VTC Spring)*, pp. 1–6, IEEE, May 2016.

[28] A. Swindlehurst, E. Ayanoglu, P. Heydari, and F. Capolino, "Millimeter-wave massive MIMO: the next wireless revolution?," *Communications Magazine, IEEE*, vol. 52, pp. 56–62, September 2014.

[29] C. Dehos, J. Gonzalez, A. De Domenico, D. Ktenas, and L. Dussopt, "Millimeter-wave access and backhauling: the solution to the exponential data traffic increase in 5G mobile communications systems?," *Communications Magazine, IEEE*, vol. 52, pp. 88–95, September 2014.

[30] S. Sun, T. Rappaport, R. Heath, A. Nix, and S. Rangan, "MIMO for millimeter-wave wireless communications: beamforming, spatial multiplexing, or both?," *Communications Magazine, IEEE*, vol. 52, pp. 110–121, December 2014.

[31] I. R. Sector, "Recommendation itu-r p. 676–10, attenuation by atmospheric gases," *International Telecommunications Union*, 2013.

[32] C. R. Anderson and T. S. Rappaport, "In-building wideband partition loss measurements at 2.5 and 60 GHz," *IEEE Transactions on Wireless Communications*, vol. 3, pp. 922–928, May 2004.

[33] G. Bartoli, R. Fantacci, K. Letaief, D. Marabissi, N. Privitera, M. Pucci, and J. Zhang, "Beamforming for small cell deployment in LTE-advanced and beyond," *IEEE Wireless Communications*, vol. 21, pp. 50–56, April 2014.

[34] S. Sun, T. S. Rappaport, T. A. Thomas, and A. Ghosh, "A preliminary 3D mm wave indoor office channel model," in *2015 International Conference on Computing, Networking and Communications (ICNC)*, pp. 26–31, IEEE, Feb. 2015.

[35] S. Hur, T. Kim, D. Love, J. Krogmeier, T. Thomas, and A. Ghosh, "Millimeter wave beamforming for wireless backhaul and access in small cell networks," *IEEE Transactions on Communications*, vol. 61, pp. 4391–4403, October 2013.

[36] H. Mehrpouyan, M. Matthaiou, R. Wang, G. Karagiannidis, and Y. Hua, "Hybrid millimeter-wave systems: a novel paradigm for hetnets," *Communications Magazine, IEEE*, vol. 53, pp. 216–221, January 2015.

[37] H. Bölcskei, D. Gesbert, C. Papadias, and A. van der Veen, *Space-Time Wireless Systems: From Array Processing to MIMO Communications*. Cambridge University Press, 2006.

[38] F. De Flaviis, L. Jofre, J. Romeu, and A. Grau, *Multiantenna Systems for MIMO Communications*. Synthesis Lectures on Antennas, Morgan & Claypool Publishers, 2013.

[39] F. B. Gross, *Smart antennas for wireless communications: with MATLAB*. McGraw-Hill New York, 2005.

[40] J. Hoydis, K. Hosseini, S. T. Brink, and M. Debbah, "Making smart use of excess antennas: Massive MIMO, small cells, and TDD," *Bell Labs Technical Journal*, vol. 18, no. 2, pp. 5–21, 2013.

[41] T. Marzetta, "Noncooperative cellular wireless with unlimited numbers of base station antennas," *IEEE Transactions on Wireless Communications*, vol. 9, pp. 3590–3600, November 2010.

[42] H. Q. Ngo, E. Larsson, and T. Marzetta, "Massive MU-MIMO downlink TDD systems with linear precoding and downlink pilots," in *Communication, Control, and Computing (Allerton), 2013 51st Annual Allerton Conference on*, pp. 293–298, Oct 2013.

[43] C. Zhang, Y. Huang, Y. Jing, S. Jin, and L. Yang, "Sum-rate analysis for massive MIMO downlink with joint statistical beamforming and user scheduling," *IEEE Transactions on Wireless Communications*, vol. 16, pp. 2181–2194, April 2017.

[44] Z. Pi and F. Khan, "An introduction to millimeter-wave mobile broadband systems," *IEEE Communications Magazine*, vol. 49, pp. 101–107, Jun 2011.

[45] H. Wei, D. Wang, H. Zhu, J. Wang, S. Sun, and X. You, "Mutual coupling calibration for multiuser massive MIMO systems," *IEEE Transactions on Wireless Communications*, vol. 15, pp. 606–619, Jan 2016.

[46] S. Yang and L. Hanzo, "Fifty Years of MIMO Detection: The Road to Large-Scale MIMOs," *IEEE Communications Surveys & Tutorials*, vol. PP, no. 99, pp. 1–1, 2015.

[47] A. I. Sulyman, A. T. Nassar, M. K. Samimi, G. R. MacCartney, T. S. Rappaport, and A. Alsanie, "Radio propagation path loss models for 5G cellular networks in the 28 GHz and 38 GHz millimeter-wave bands," *IEEE Communications Magazine*, vol. 52, pp. 78–86, Sept. 2014.

[48] M. K. Samimi and T. S. Rappaport, "3-D Millimeter-Wave Statistical Channel Model for 5G Wireless System Design," *IEEE Transactions on Microwave Theory and Techniques*, vol. 64, pp. 2207–2225, Jul 2016.

[49] P. V. Amadori and C. Masouros, "Low RF-Complexity Millimeter-Wave Beamspace-MIMO Systems by Beam Selection," *IEEE Transactions on Communications*, vol. 63, pp. 2212–2223, June 2015.

[50] J. Wang, H. Zhu, L. Dai, N. J. Gomes, and J. Wang, "Low-complexity beam allocation for switched-beam based multiuser massive MIMO systems," *IEEE Transactions on Wireless Communications*, vol. 15, pp. 8236–8248, Dec 2016.

[51] C. Masouros and G. Zheng, "Power efficient downlink beamforming optimization by exploiting interference," in *2015 IEEE Global Communications Conference (GLOBECOM)*, pp. 1–6, Dec 2015.

[52] J. Winters, "Smart antennas for wireless systems," *IEEE Personal Communications*, vol. 5, pp. 23–27, Feb 1998.

[53] R. W. Heath, N. Gonzalez-Prelcic, S. Rangan, W. Roh, and A. M. Sayeed, "An Overview of Signal Processing Techniques for Millimeter Wave MIMO Systems," *IEEE Journal of Selected Topics in Signal Processing*, vol. 10, pp. 436–453, April 2016.

[54] M. Gkizeli and G. N. Karystinos, "Maximum-SNR Antenna Selection Among a Large Number of Transmit Antennas," *IEEE Journal of Selected Topics in Signal Processing*, vol. 8, pp. 891–901, Oct. 2014.

[55] J. Kim and A. Molisch, "Fast millimeter-wave beam training with receive beamforming," *IEEE Journal of Communications and Networks*, vol. 16, pp. 512–522, Oct 2014.

[56] T. E. Bogale, L. B. Le, A. Haghighat, and L. Vandendorpe, "On the Number of RF Chains and Phase Shifters, and Scheduling Design With Hybrid Analog-Digital Beamforming," *IEEE Transactions on Wireless Communications*, vol. 15, pp. 3311–3326, May 2016.

[57] A. Alkhateeb, G. Leus, and R. W. Heath, "Limited Feedback Hybrid Precoding for Multi-User Millimeter Wave Systems," *IEEE Transactions on Wireless Communications*, vol. 14, pp. 6481–6494, Nov. 2015.

[58] R. Mendez-Rial, C. Rusu, N. Gonzalez-Prelcic, A. Alkhateeb, and R. W. Heath, "Hybrid MIMO Architectures for Millimeter Wave Communications: Phase Shifters or Switches?," *IEEE Access*, vol. 4, pp. 247–267, 2016.

[59] S. Buzzi and C. D'Andrea, "Are mmwave low-complexity beamforming structures energy-efficient? Analysis of the downlink MU-MIMO," in *2016 IEEE Globecom Workshops (GC Wkshps)*, pp. 1–6, Dec 2016.

[60] K. Roth, H. Pirzadeh, A. L. Swindlehurst, and J. A. Nossek, "A comparison of hybrid beamforming and digital beamforming with low-resolution adcs for multiple users and imperfect CSI," *IEEE Journal of Selected Topics in Signal Processing*, vol. PP, no. 99, pp. 1–1, 2018.

[61] J. Hoydis, S. ten Brink, and M. Debbah, "Massive MIMO in the UL/DL of Cellular Networks: How Many Antennas Do We Need?," *IEEE Journal on Selected Areas in Communications*, vol. 31, pp. 160–171, Feb. 2013.

[62] O. K. Rayel, G. Brante, J. L. Rebelatto, R. D. Souza, and M. A. Imran, "Energy efficiency-spectral efficiency trade-off of transmit antenna selection," *IEEE Transactions on Communications*, vol. 62, pp. 4293–4303, Dec 2014.

[63] K. Dong, N. Prasad, X. Wang, and S. Zhu, "Adaptive antenna selection and tx/rx beamforming for large-scale mimo systems in 60 ghz channels," *EURASIP Journal on Wireless Communications and Networking*, vol. 2011, p. 59, Aug 2011.

[64] Z. Liu, W. Du, and D. Sun, "Energy and spectral efficiency tradeoff for massive MIMO systems with transmit antenna selection," *IEEE Transactions on Vehicular Technology*, vol. 66, pp. 4453–4457, May 2017.

[65] X. Zhai, Y. Cai, Q. Shi, M. Zhao, G. Y. Li, and B. Champagne, "Joint Transceiver Design With Antenna Selection for Large-Scale MU-MIMO mmWave Systems," *IEEE Journal on Selected Areas in Communications*, vol. 35, pp. 2085–2096, Sept 2017.

[66] C. Pan, H. Zhu, N. J. Gomes, and J. Wang, "Joint precoding and RRH selection for user-centric green MIMO C-RAN," *IEEE Transactions on Wireless Communications*, vol. 16, pp. 2891–2906, May 2017.

[67] R. Chen, J. G. Andrews, and R. W. Heath, "Efficient transmit antenna selection for multiuser mimo systems with block diagonalization," in *IEEE GLOBECOM 2007 - IEEE Global Telecommunications Conference*, pp. 3499–3503, Nov 2007.

[68] H. Li, L. Song, and M. Debbah, "Energy Efficiency of Large-Scale Multiple Antenna Systems with Transmit Antenna Selection," *IEEE Transactions on Communications*, vol. 62, pp. 638–647, Feb. 2014.

[69] H. Lei, J. Zhang, K. H. Park, P. Xu, I. S. Ansari, G. Pan, B. Alomair, and M. S. Alouini, "On secure NOMA systems with transmit antenna selection schemes," *IEEE Access*, vol. 5, pp. 17450–17464, 2017.

[70] J. Zhang, Y. Huang, J. Wang, B. Ottersten, and L. Yang, "Per-antenna constant envelope precoding and antenna subset selection: A geometric approach," *IEEE Transactions on Signal Processing*, vol. 64, pp. 6089–6104, Dec 2016.

[71] P. H. Lin and S. H. Tsai, "Performance analysis and algorithm designs for transmit antenna selection in linearly precoded multiuser MIMO systems," *IEEE Transactions on Vehicular Technology*, vol. 61, pp. 1698–1708, May 2012.

[72] Z. Wang and L. Vandendorpe, "Antenna selection for energy efficient MISO systems," *IEEE Communications Letters*, vol. 21, pp. 2758–2761, Dec 2017.

[73] H. Li, L. Song, and M. Debbah, "Energy efficiency of large-scale multiple antenna systems with transmit antenna selection," *IEEE Transactions on Communications*, vol. 62, pp. 638–647, February 2014.

[74] B. C. Lim, W. A. Krzymien, and C. Schlegel, "Transmit antenna selection for sum rate maximization in transmit zero-forcing beamforming," in *2006 10th IEEE Singapore International Conference on Communication Systems*, pp. 1–5, Oct 2006.

[75] S. K. Mishra and K. D. Kulat, "Reduced feedback rate schemes for transmit antenna selection with alamouti coding," *IEEE Access*, vol. 6, pp. 10028–10040, 2018.

[76] R. Husbands, Q. Z. Ahmed, F. A. Khan, P. Lazaridis, and I. Glover, "Transmit antenna selection for massive mimo systems," *Proceedings of the XXXI-Ind International Union of Radio Science General Assembly & Scientific Symposium (URSI GASS), (Montreal, 19-26 August 2017)*, August 2017.

[77] S. Martello and P. Toth, *Knapsack problems: algorithms and computer implementations*. Wiley-Interscience series in discrete mathematics and optimization, J. Wiley & Sons, 1990.

[78] H. Godrich, A. P. Petropulu, and H. V. Poor, "Sensor Selection in Distributed Multiple-Radar Architectures for Localization: A Knapsack Problem Formulation," *IEEE Transactions on Signal Processing*, vol. 60, pp. 247–260, Jan. 2012.

[79] R. Husbands, Q. Z. Ahmed, and J. Wang, "Transmit antenna selection for massive MIMO: a knapsack problem formulation," in *IEEE ICC 2017 Wireless Communications Symposium (ICC'17 WCS)*, (Paris, France), pp. 2313–2318, May 2017.

[80] B. Mondal, T. Thomas, E. Visotsky, F. Vook, A. Ghosh, Y.-H. Nam, Y. Li, J. Zhang, M. Zhang, Q. Luo, Y. Kakishima, and K. Kitao, "3D channel model in 3GPP," *IEEE Communications Magazine*, vol. 53, pp. 16–23, Mar 2015.

[81] T. Bai, A. Alkhateeb, and R. Heath, "Coverage and capacity of millimeter-wave cellular networks," *IEEE Communications Magazine*, vol. 52, pp. 70–77, Sep 2014.

[82] W. Lee, S.-R. Lee, H.-B. Kong, S. Lee, and I. Lee, "Downlink Vertical Beamforming Designs for Active Antenna Systems," *IEEE Transactions on Communications*, vol. 62, pp. 1897–1907, Jun 2014.

[83] A. F. Molisch and M. Z. Win, "MIMO systems with antenna selection," *IEEE Microwave Magazine*, vol. 5, pp. 46–56, Mar 2004.

[84] S. Sanayei and A. Nosratinia, "Antenna selection in MIMO systems," *IEEE Communications Magazine*, vol. 42, pp. 68–73, Oct 2004.

[85] X. Gao, L. Dai, S. Han, C. L. I, and R. W. Heath, "Energy-Efficient Hybrid Analog and Digital Precoding for MmWave MIMO Systems With Large Antenna Arrays," *IEEE Journal on Selected Areas in Communications*, vol. 34, pp. 998–1009, Apr. 2016.

[86] P. V. Amadori and C. Masouros, "Interference-driven antenna selection for massive multiuser mimo," *IEEE Transactions on Vehicular Technology*, vol. 65, pp. 5944–5958, Aug 2016.